Commun Nonlinear Sci Numer Simulat 130 (2024) 107788

Contents lists available at ScienceDirect

Communications in Nonlinear Science and Numerical Simulation

journal homepage: www.elsevier.com/locate/cnsns

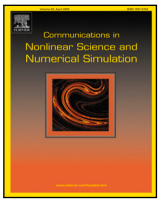

Research paper

On–off intermittency in population outbreaks: Reactive equilibria and propagation on networks

Angela Monti [a,*], Fasma Diele [a], Carmela Marangi [a], Antonello Provenzale [b]

[a] Istituto per le Applicazioni del Calcolo 'M. Picone', National Research Council (CNR), via G. Amendola 122/D, Bari, 70126, Italy
[b] Institute of Geosciences and Earth Resources (IGG), National Research Council (CNR), Via Giuseppe Moruzzi 1, Pisa, 56124, Italy

ARTICLE INFO

Keywords:
On–off intermittency
Population outbreaks
Population dynamics
Networks

ABSTRACT

Ecological systems are subject to environmental variability and fluctuations: understanding the role of such stochastic perturbations in inducing on–off intermittency is the central motivation for this study. This research extends the exploration of parameters leading to the emergence of on–off intermittency within a discrete Beddington-Free-Lawton host-parasitoid model. We introduce random perturbation factors that impact both the grazing intensity and the growth rate of the host population. An intriguing aspect of this study is the numerical evidence of the reactivity of the free-parasitoid fixed point as a route to on–off intermittency. This finding is significant because it sheds light on how stable ecological equilibria can transition into intermittency before progressing toward chaotic behaviour. Moreover, our study explores the host-parasitoid coupling within the Beddington-Free-Lawton model when it is applied to a complex network, a significant framework for modelling ecological interactions. The paper reveals that such network-based interactions induce parasitoid bursts that are not observed in a single population scenario.

1. Introduction

In dynamical systems, chaotic intermittency is the term used to describe the switching behaviour between periodic, quasi-periodic, and chaotic regimes [1]. Classically, chaotic intermittency has been classified into three different types called I, II, and III, according to the system's Floquet multipliers or the eigenvalues in the local Poincaré map [2]. An intermittent behaviour of the classical type is a route to chaos characterized by so-called laminar phases when the behaviour is regular (e.g., stationary to quasi-periodic) for a finite time, interrupted by chaotic bursts. There are other types of intermittency, such as crisis-induced intermittency [3], or Type-V and Type-X intermittency [2].

In this paper, we are interested in a special case of intermittency, called on–off intermittency [4–6]. On–off intermittency has found applications in modelling various phenomena, including the solar cycle [7,8], neurophysiological dynamics [9,10], earthquake occurrences [11], and electronic circuits [12]. The properties of this form of intermittency have been studied from the perspective of time series analysis and coupled system dynamics [13–15]. A comparison with other forms of intermittency was conducted in [14]. More recently, on–off intermittency models have been employed to describe sudden population outbreaks in host-parasitoid populations, addressing critical ecological questions that warrant further investigation [16–21].

To induce this specific intermittent behaviour, two key components are required: an invariant object and a mechanism that permits orbits to approach and depart from a small region around the invariant object without transitioning into the basin of

* Corresponding author.
E-mail address: a.monti@ba.iac.cnr.it (A. Monti).

https://doi.org/10.1016/j.cnsns.2023.107788
Received 27 July 2023; Received in revised form 10 December 2023; Accepted 14 December 2023
Available online 16 December 2023

attraction of another, potentially existing, invariant object. The simplest discrete dynamical system having these elements can be written as [5]:

$$\mathbf{X}_{t+1} = \mathbf{X}_t + \mathbf{f}(\mathbf{X}_t, \nu(\mathbf{Y}_t)) \tag{1}$$

where ν is a control parameter and $\mathbf{Y}_t$ is taken from a random or deterministic chaotic process. In Eq. (1) the evolution of $\mathbf{Y}_t$ does not depend on $\mathbf{X}_t$ but the $\mathbf{X}_t$ evolution depends on $\mathbf{Y}_t$. Suppose that the simplest invariant object, i.e. a fixed point $\mathbf{X}^*$, satisfies

$$\mathbf{f}(\mathbf{X}^*, \nu(\mathbf{Y}_t)) = \mathbf{0}, \quad \forall\, \nu(\mathbf{Y}_t).$$

In other words, it remains unaffected by the values assumed by the control parameter $\nu = \nu(\mathbf{Y}_t)$. However, it becomes unstable when the control parameter exceeds a critical threshold, denoted as ν_c. If $\mathbf{Y}_t$ moves between two regions where ν fluctuates above and below the critical control parameter ν_c and, if the time spent in both regions is appropriately balanced, then on–off intermittency can arise around the fixed point $\mathbf{X}^*$. Hence, the fundamental process behind on–off intermittency is the reiterated modification of one dynamical variable across a bifurcation point of another dynamical variable.

As we are interested in representing the climate and environmental variability effects into qualitative ecological models (e.g. [22]), we suppose that $\mathbf{Y}_t$ is taken from a random process which represents stochastic perturbation in some of the main model parameters. In [21], such parametric perturbation has lead to the occurrence of on–off intermittency in the discrete Beddington-Free-Lawton model [23], a feature that qualitatively describes abrupt changes in the host-parasitoid population sizes [24].

In this work, we perform the investigation of parameters inducing on–off intermittency in an extended version of the discrete Beddington-Free-Lawton model previously examined in [21]. Our model introduces random forcing factors that impact not only the grazing intensity but also the growth rate of the host population. These stochastic elements play a crucial role in influencing the onset of on–off intermittency.

Starting from the existing literature, we introduce the concept of reactivity of a fixed point within the statistical framework, underscoring its significance as an essential prerequisite for the emergence of on–off intermittency. The analysis yields numerical evidence that equilibrium reactivity is a necessary condition for the emergence of on–off intermittency. This perspective sheds light on a crucial dimension of the dynamics that has remained unexplored in previous studies.

Furthermore, we investigate the consequences of employing a complex network comprised of Beddington-Free-Lawton discrete maps to model host-parasitoid interactions. This investigation leads to the induction of bursting behaviour in the parasitoid population, achieved through a suitable, non-diffusive coupling between the host and parasitoid populations. The use of complex networks together with Beddington-Free-Lawton discrete maps for modelling host-parasitoid interactions, which is inherently more complex than single population dynamics, underlines our innovative approach to understand on–off intermittency in ecological systems.

The paper is organized as follows. In Section 2, we study the onset of on–off intermittency when parameters randomly vary, e.g. the grazing intensity (Section 2.1) or the host growth rate (Section 2.2). In particular, in Section 2.3, we investigate the reactivity as a necessary condition for the emergence of on–off intermittency. Then, in Section 3, we analyse the host-parasitoid coupling of discrete maps on a complex network with ring structure. We show that a not-diffusive coupling induces parasitoid bursts that are not observed in a single population. In Section 4, we summarize our findings and propose potential directions for future research. Finally, in Appendix, we provide the qualitative analysis of the Beddington-Free-Lawton model in the full-deterministic case: we study its fixed points (Appendix A.1) together with their stability (Appendix A.2) and bifurcation (Appendix A.3) properties. We also recall the classical notions of reactivity and resilience in Appendix A.4.

2. The onset of on–off intermittency in the Beddington-Free-Lawton model

The Beddington-Free-Lawton model is represented by the following equations:

$$\begin{aligned} N_{t+1} &= \delta\, N_t \exp\left[r\left(1 - \frac{N_t}{K}\right) - \beta\, P_t\right] \\ P_{t+1} &= b\, N_t \left[1 - \exp\left(-a\, P_t\right)\right]. \end{aligned} \tag{2}$$

It is important to highlight that, in contrast to the model presented in [21], the model (2) is more general, as it allows for distinct values for the constant rates a and β.

On–off intermittency in host dynamics can emerge in Beddington's model by incorporating stochastic variations in some parameters [21]. The literature has demonstrated that intermittent behaviour typically emerges as an initial destabilization of equilibria, acting as a route to chaotic dynamics [6,18,21]. Therefore, in a general sense, a linear stability analysis at the fixed points is essential for identifying the parameters responsible for the onset of on–off intermittency. As first step we reduce the number of parameters by performing a change of variables. We set $Y = a\,P$ and $X = a\,b\,N$, $c = \beta/a$ and $k = a\,b\,K$, resulting in the following equations:

$$\begin{aligned} X_{t+1} &= \delta\, X_t \exp\left[r\left(1 - \frac{X_t}{k}\right) - c\, Y_t\right] \\ Y_{t+1} &= X_t \left[1 - \exp\left(-Y_t\right)\right]. \end{aligned} \tag{3}$$

In the next section, we conduct the analysis regarding the emergence of on–off intermittency induced by stochastic variations in the intensity of grazing by the host. This is modelled by allowing the parameter δ in (3) to vary over time.

For the sake of completeness and to facilitate a comparative analysis between the deterministic and stochastic cases, in Appendix we have conducted a local stability analysis of model (2) and we have examined bifurcations in the full deterministic case.

2.1. δ_t randomly varying

For all $t \geq 0$ we define $\delta_t = \delta + (D - \delta)\,\epsilon_t$, where $0 < \delta \leq D$ and ϵ_t is a random variable in the interval $[0, 1]$ with uniform distribution. We analyse the model

$$\begin{aligned} X_{t+1} &= \delta_t\, X_t\, \exp\left[r\left(1 - \frac{X_t}{k}\right) - c\, Y_t\right] \\ Y_{t+1} &= X_t\left[1 - \exp\left(-Y_t\right)\right]. \end{aligned} \tag{4}$$

Setting $\rho_t := r + log(\delta_t)$ and $k_r := k/r$, the model (4) can be written as

$$\begin{aligned} X_{t+1} &= X_t\, \exp\left(\rho_t - \frac{X_t}{k_r} - c\, Y_t\right) \\ Y_{t+1} &= X_t\left[1 - \exp\left(-Y_t\right)\right]. \end{aligned} \tag{5}$$

The model (5) has only one extinction fixed point $P_0 = (0, 0)$. The linearized system at P_0 is given by $\eta_{t+1} = J_0^{(t)}\,\eta_t$ with

$$J_0^{(t)} = \begin{bmatrix} \exp(\rho_t) & 0 \\ 0 & 0 \end{bmatrix} \tag{6}$$

so that

$$\eta_t = \overset{\curvearrowleft}{\prod_{i=0}^{t-1}} J_0^{(i)}\,\eta_0 = \begin{bmatrix} \prod_{i=0}^{t-1}\exp(\rho_i) & 0 \\ 0 & 0 \end{bmatrix}\eta_0$$

where $\overset{\curvearrowleft}{\prod_{i=0}^{t-1}} J_0^{(i)} = J_0^{(t-1)} \cdot J_0^{(t-2)} \cdot \ldots \cdot J_0^{(0)}$. The stability of the linearized system is determined by

$$\Lambda_T = \lim_{t\to\infty}\frac{1}{t}\,\ln\left(\max_{\|\mu_0\|\neq 0}\frac{\|\mu_t\|}{\|\mu_0\|}\right)$$

that, if we consider the Euclidean norm on vectors, is computed by using the spectral norm $|||\ \cdot\ |||$ of $\overset{\curvearrowleft}{\prod_{i=0}^{t-1}} J_0^{(i)}$. In other words,

$$\Lambda_T = \lim_{t\to\infty}\frac{1}{t}\,\ln\,\sigma_{max}\left(\overset{\curvearrowleft}{\prod_{i=0}^{t-1}} J_0^{(i)}\right)$$

where σ_{max} denotes the largest singular value of the matrix. Since $\overset{\curvearrowleft}{\prod_{i=0}^{t-1}} J_0^{(i)}$ is a diagonal matrix with eigenvalues $\lambda_1 = \prod_{i=0}^{t-1}\exp(\rho_i)$ and $\lambda_2 = 0$, then

$$\Lambda_T = \lim_{t\to\infty}\frac{1}{t}\,\ln\left|\prod_{i=0}^{t-1}\exp(\rho_i)\right| = \lim_{t\to\infty}\frac{1}{t}\sum_{i=0}^{t-1}\rho_i = \lim_{t\to\infty}\langle\rho\rangle$$

where $\langle\rho\rangle = \frac{1}{t}\sum_{i=0}^{t-1}\rho_i$. According to the law of large numbers, we can compute $\lim_{t\to\infty}\langle\rho\rangle$ through the phase-space average as in [6]. Since $\rho_t = \rho_t(\epsilon)$ and ϵ is a random variable in $[0, 1]$ with uniform distribution, then

$$\Lambda_T = \int_0^1 \rho_t(\epsilon)\, d\epsilon.$$

The fixed point P_0 is stable if $\Lambda_T < 0$ and unstable if $\Lambda_T > 0$. Note that when $D = \delta$, we revert to the deterministic case where $\delta_t = \delta + (D - \delta)\epsilon_t = \delta$ and $\rho_t = r + \log(\delta) = \rho$. Consequently,

$$\Lambda_T = \int_0^1 \rho\ d\epsilon = \rho.$$

This clearly aligns with the stability condition of P_0 as presented in Theorem 2 in Appendix. More generally, when $D > \delta$, the extinction equilibrium P_0 is stable if

$$\Lambda_T = \int_0^1 (r + \ln(\delta + (D - \delta)\,\epsilon))\, d\epsilon = r\ -1\ + log\frac{D^{\frac{D}{D-\delta}}}{\delta^{\frac{\delta}{D-\delta}}} < 0.$$

The stability curve, corresponding to $\Lambda_T = 0$, is determined by the function $D_c = f(\delta)$, which is implicitly defined by the relationship:

$$D_c^{\frac{D_c}{D_c-\delta}} = \exp(1 - r)\,\delta^{\frac{\delta}{D_c-\delta}}. \tag{7}$$

This curve is depicted on the left side of Fig. 1 for the case $r = 3$. Again notice that, for δ tending to $exp(-r) \approx 0.0498$, the function $f(\delta)$ tends to intercept the straight line $D = \delta$ and we recover the critical deterministic case, corresponding to $\rho = 0$ i.e. $r + log(\delta) = 0 \iff \delta = exp(-r)$ (see Theorem 2 in Appendix A.2).

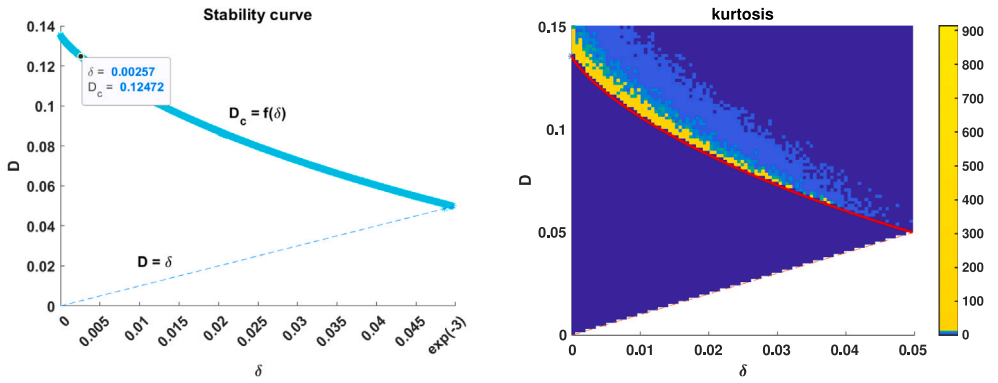

Fig. 1. Left panel: the stability curve of P_0 (cyan solid line) given by $D_c = f(\delta)$ in (7) is plotted for $r = 3$ in the (δ, D) plane. In the same figure, the bisector line $D = \delta$ (cyan dashed line), which corresponds to the fully deterministic case, intersects the curve D_c at $\delta = \exp(-r)$. Right panel: kurtosis values for the host population in the (δ, D) plane above the bisector line $D = \delta$. In the same figure, the stability curve of P_0 is represented by a red solid line. The kurtosis is greater than 3 above and very close to the stability curve of P_0. The stability and reactivity curves overlap (see Section 2.3).

From Fig. 1, it can be observed that for $r = 3$ and $\delta = 0.0025701$, the critical value is $D_c \approx 0.12472$. Next, setting the other parameter values to $c = 1$ and $k = 4.9$, we run a simulation for 10^5 time steps using the model (5), starting with random initial conditions. The appearance of an intermittent behaviour for host-population X has been observed for certain values of $D \geq D_c$, very close to D_c, as depicted in Fig. 2, where we plot the last 1000 time steps of the simulation. To verify whether the observed dynamics correspond to on–off intermittency, we use three statistical tools: the kurtosis, the probability distribution of the off phases and the power spectrum.

The kurtosis of a time series is a statistical quantity that is able to detect infrequent extreme deviations. Given a time series X_t, the kurtosis is defined as

$$\frac{\langle \left(X_t - \langle X_t \rangle\right)^4 \rangle}{\langle \left(X_t - \langle X_t \rangle\right)^2 \rangle^2}$$

and it quantifies extreme values of the distribution compared to a normal (Gaussian) distribution. Values of kurtosis much greater than 3 indicate heavier tails (more extreme values) than a normal distribution (see e.g.[15]). In our simulations we compute the kurtosis by using the Matlab default function `kurtosis`.

As a second method, for confirming the existence of on–off intermittency, we examine the probability distribution of the off-phases. In a study conducted in [6], it was observed that when on–off intermittency begins, the probability density function describing the duration of off-stages follows a power law with an exponent of $-\frac{3}{2}$. In our simulation, to measure the duration of the off-phases, we first specify a threshold below which the system is considered to be off. Then, we compute the time intervals corresponding to off stages, by considering consecutive time steps at which the system is off. In other words, the duration of an off-stage can also be viewed as the time step between two consecutive on-stages. We then compute the length of each time interval. The probability of having an off phase of duration $\bar{t}$ is given by the ratio between the number of intervals of length $\bar{t}$ and the number of all the time intervals.[1]

As the third and final method for proving the presence of on–off intermittency, we employ power spectrum analysis. In [14], the authors show that the logarithmic slope of the power spectrum is negative for on–off intermittency, whereas it is null or positive for noisy chaotic, non intermittent dynamics.

We employ the three aforementioned criteria to assess whether the observed dynamics in Fig. 2 represent on–off intermittency. In Fig. 3, we present evidence of the logarithmic decrease in the (average) power spectrum and the slope of the distribution of off phases for $\delta = 0.0025701$ and the three different cases represented in the left panel of Fig. 2 i.e. $D = D_c = 0.12472$, $D = 0.126$, and $D = 0.13$. The corresponding kurtosis values are 621.8507, 85.9402, and 21.8620, respectively, indicating on–off intermittency. Furthermore, when $D = 0.2 \gg D_c$, the dynamics of the host population becomes chaotic (Fig. 2, on the right) leading to the loss of on–off intermittency behaviour confirmed by the kurtosis value of $2.5379 < 3$.

To generalize our analysis and determine the appearance of on–off intermittency, we localize the pairs (δ, D) for which the host population has kurtosis greater than 3. In Fig. 1, on the right, we show that the region of possible on–off intermittency lies in the region of P_0 instability, close to the stability curve. This confirms what has been observed in literature for a single equation (see e.g. Fig. 3 in [18]).

In the next section, our emphasis is on the emergence of intermittency resulting from stochastic variations in the intensity of the host growth rate r in (3). It is worth mentioning that the study in [21] did not explore the emergence caused by stochastic variations in r. Therefore, the analysis presented here represents a new investigation into this aspect.

[1] In order to numerically reproduce the probability distribution of off-phases, Matlab codes have been uploaded on https://github.com/CnrIacBaGit/OnOffIntermittency.

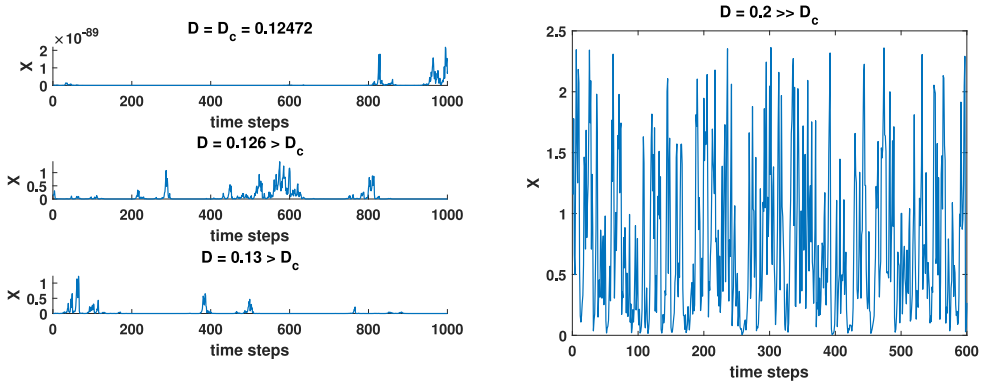

Fig. 2. δ_t randomly varying: on the left, the temporal evolution of the host population X is shown over the last 1000 time steps, obtained by a simulation of 10^5 time steps. The parameter values are set to $c = 1$, $k = 4.9$, $r = 3$, and $\delta = 0.0025701$. Intermittent behaviour becomes evident for values of $D = 0.126$ (second row) and $D = 0.13$ (third row), both of which are above the critical value $D_c = 0.12472$ (first row). Right panel: a simulation is conducted over 10^5 time steps and we report the last 600, with $D = 0.2 \gg D_c$. Other parameters are set as in the left panel. The loss of host on–off intermittency is observed, with the system transitioning to chaotic behaviour.

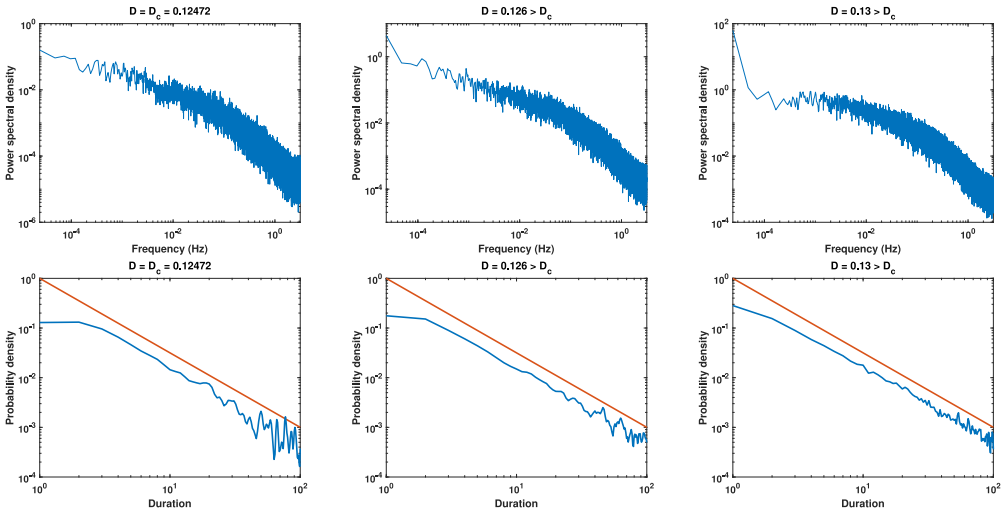

Fig. 3. δ_t randomly varying: statistical verification of host population on–off intermittency shown in Fig. 2. Parameters $D = D_c = 0.12472$ (first column), $D = 0.126$ (second column) $D = 0.13$ (third column). The other parameters are set as in Fig. 2. Upper panels report the power spectra, lower panels show the distribution of the off phases (the red line indicates a logarithmic slope $-3/2$). As kurtosis values are 621.8507, 85.9402 and 21.8620, all the three statistic tools confirm the arising of on–off intermittency.

2.2. r_t randomly varying

We consider $\delta = 1$ and for all $t \geq 0$ suppose that $r_t = r + (R - r)\epsilon_t$, where $0 < r \leq R$ and ϵ_t is a random variable in $[0, 1]$ with uniform distribution. Taking into account that $\rho = r + log(\delta) = r + log(1) = r$, the model

$$\begin{aligned} X_{t+1} &= X_t \exp\left[r_t\left(1 - \frac{X_t}{k}\right) - c\, Y_t\right] \\ Y_{t+1} &= X_t\left[1 - \exp\left(-Y_t\right)\right] \end{aligned} \tag{8}$$

admits the extinction fixed point $P_0 = (0, 0)$ and the free-parasitoid fixed point $P_1 = (k, 0)$.

The linearized system at the fixed point $P_0 = (0, 0)$ is given by $\eta_{t+1} = J_0(t)\,\eta_t$ with

$$J_0^{(t)} = \begin{bmatrix} \exp(r_t) & 0 \\ 0 & 0 \end{bmatrix}$$

so that

$$\eta_t = \overset{\curvearrowleft}{\prod_{i=0}^{t-1}} J_0^{(i)}\,\eta_0 = \begin{bmatrix} \prod_{i=0}^{t-1}\exp(r_i) & 0 \\ 0 & 0 \end{bmatrix}\eta_0.$$

As before, the stability of the linearized system is determined by

$$\Lambda_T = \lim_{t\to\infty}\frac{1}{t}\ln\left|\prod_{i=0}^{t-1}\exp(r_i)\right| = \lim_{t\to\infty}\frac{1}{t}\sum_{i=0}^{t-1} r_i = \lim_{t\to\infty}\langle r\rangle$$

that can be computed through the phase-space average

$$\Lambda_T = \int_0^1 r + (R-r)\epsilon\, d\epsilon = \frac{R+r}{2} > 0,$$

proving that P_0 is always unstable. When $R = r$, it holds that $r_t = r + (R-r)\epsilon_t = r$ and we recover the deterministic scenario. This implies:

$$\int_0^1 r\, d\epsilon = r > 0$$

and confirms the instability of P_0, even in the deterministic framework. Indeed, the stability properties of P_0, given in Theorem 2 in Appendix A.2, would require $\rho = r + log(\delta) < 0$ which, for $\delta = 1$, would ask for $r < 0$.

Consider now the Jacobian matrix at $P_1 = (k, 0)$

$$J_1^{(t)} := \begin{bmatrix} 1-r_t & -k\,c \\ 0 & k \end{bmatrix} \tag{9}$$

and the matrix $\overset{\curvearrowleft}{\prod_{i=0}^{t-1}} J_i^{(1)}$ that results upper triangular with eigenvalues $\lambda_1 = \prod_{i=0}^{t-1}(1-r_i)$ and $\lambda_2 = k^t$. The evaluation of its largest singular value is not a trivial task; for this reason, we prefer to use a different quantity $\tilde{\Lambda}_T$, equivalent in sign to Λ_T, for determining the stability of P_1:

$$\tilde{\Lambda}_T = \lim_{t\to\infty}\frac{1}{t}\ln\max_i\left|\lambda_i\left(\overset{\curvearrowleft}{\prod_{i=0}^{t-1}} J_i^{(1)}\right)\right|.$$

Under the hypothesis that $0 < k < r - 1 \le 1$, the long-term behaviour of η_t is determined by

$$\tilde{\Lambda}_T = \lim_{t\to\infty}\frac{1}{t}\ln\prod_{i=0}^{t-1}(r_i - 1) = \lim_{t\to\infty}\frac{1}{t}\sum_{i=0}^{t-1}\ln(r_i - 1) = \lim_{t\to\infty}\langle\ln(r-1)\rangle$$

that can be approximated as

$$\tilde{\Lambda}_T = \int_0^1 \ln(r + (R-r)\epsilon - 1)\, d\epsilon = \ln\frac{(R-1)^{\frac{R-1}{R-r}}}{(r-1)^{\frac{r-1}{R-r}}} - 1.$$

The stability curve $R_c = f(r)$, associated with $\tilde{\Lambda}_T = 0$, is implicitly determined by the relation

$$(R_c - 1)^{\frac{R_c-1}{R_c-r}} = \exp(1)\,(r-1)^{\frac{r-1}{R_c-r}} \tag{10}$$

and is depicted on the left side of Fig. 4. For instance, we focus on the point along the stability curve corresponding to $r = 1.508$ and seek to verify whether $R_c = 2.59131$ marks the threshold between stable and unstable dynamics in the model (8), when $0 < k < r - 1 \le 1$. To numerically confirm this, we plot orbit diagrams for model (8) with $c = 1$, $r = 1.508$, and $k = 0.49$. The host attractors are displayed on the left side of Fig. 6. We observe that, while gradually varying R from 1.508 to 7, the free-parasitoid fixed point solution becomes unstable at $R \approx R_c = 2.59131$ and the long-term solution transitions into a chaotic regime.

In the right panel of Fig. 4, we can observe the emergence of host intermittency for a value of $R = 2.6$, which is slightly above the critical value R_c. Once again, we confirm the presence of on–off intermittency by examining the power spectrum and the distribution of the off phases, as shown in Fig. 5 on the left and right, respectively. Furthermore, the kurtosis value of 35.28, for the host population, is significantly greater than 3, which is consistent with the characteristics of on–off intermittent behaviour.

It is worth noting that we have not considered stochastic perturbations of the parameter k, because changing the value of k also results in an alteration of the fixed point $P_1 = (k, 0)$. Consequently, according to the dynamic description provided in the Introduction, stochastic perturbations in k will not correspond to an on–off intermittency scenario.

For the sake of completeness, let us explore the effect of the destabilization of the fixed point $P_1 = (k, 0)$ for different values of the parameter k. We recall that k corresponds to an eigenvalue of the Jacobian matrix (9), so we consider values of the parameter k slightly above the critical value of 1. We aim to investigate the impact of combined destabilization on the host-parasitoid dynamics, resulting from the stochastic variation of the parameter r and instability associated with $k > 1$.

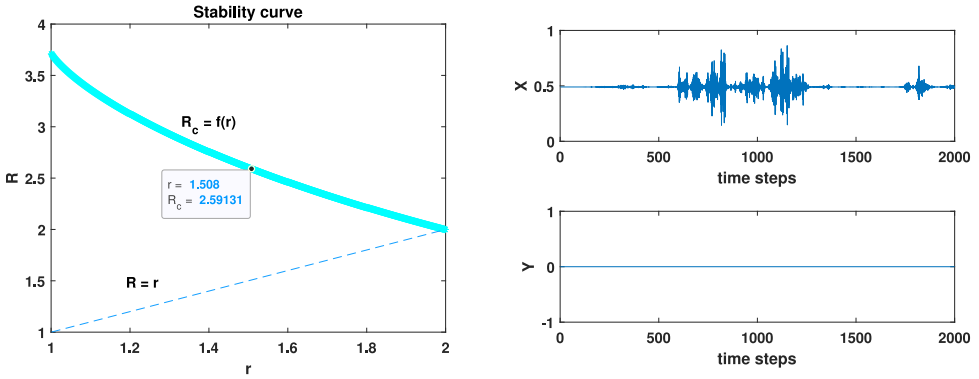

Fig. 4. r_t randomly varying: on the left, the stability curve of P_1 (cyan solid line) given by $R_c = f(r)$ in (10) is plotted in the (r, R) plane. In the same figure, the bisector line $R = r$ (cyan dashed line), which corresponds to the fully deterministic case, intersects the curve R_c at $r = 2$. Right plot: the parasitoid population Y (second row) maintains a null state during the intermittent behaviour of the host population X (first row) over a span of 2000 time steps. Parameters $c = 1$, $r = 1.508$, $k = 0.49$, $R = 2.6$.

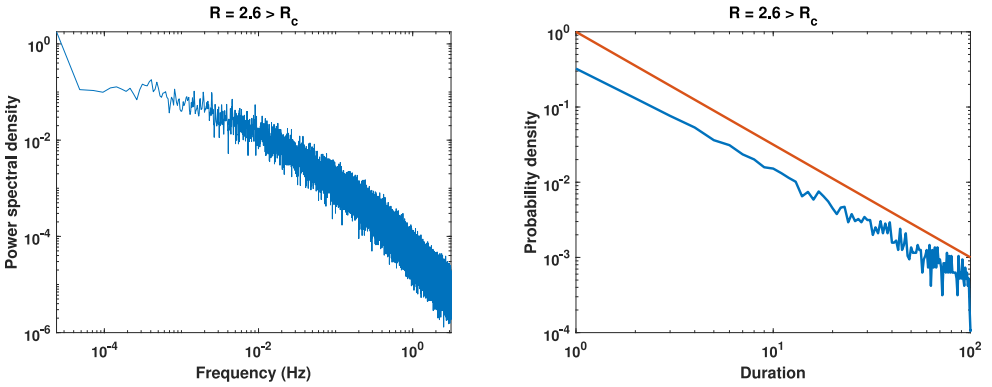

Fig. 5. r_t randomly varying: statistical verification of on–off intermittency for the host population, shown in the right panel of Fig. 4. The left plot shows the power spectrum, while the right panel displays the distribution of the off phases. The kurtosis value is 35.28. These three statistical tools provide confirmation of the on–off nature of host population intermittency around the fixed point P_1.

In the right panel of Fig. 6, we can observe that the parasitoid attractor at the null value remains stable for $k < 1$. However, when $k \geq 1$, the orbit diagrams depicting host-parasitoid attractors for the model (8) reveal that the invariant null parasitoid state may destabilize. This is illustrated in Fig. 7 on the right, where we present the orbit diagrams illustrating parasitoid attractors for $k = 1.0093$, with $r = 1.508$, $c = 1$ and R varying from 1.508 to 7. It becomes evident that the parasitoid attractor assumes non-null values for $R < R_p = 2.605$. Notably, beyond this critical value, despite $k > 1$, $Y = 0$ remains the sole attractor for parasitoid dynamics.

For $r = 1.508$ and values of R within the range $R_c < R < R_p$, host on–off intermittency persists, even when k is slightly greater than the critical value of 1, as illustrated in Fig. 8 (first row). The kurtosis values for the host population are 17.1848 (for $k = 1.011$) and 14.0109 (for $k = 1.0093$), which confirm the presence of on–off intermittency. Also the power spectrum and the distribution of the off phases, that we do not show here, guarantee the onset of on–off intermittency. In this regime, we also observe irregular behaviour in parasitoids (Fig. 8, second row), and we expect that this behaviour is not of an on–off intermittency nature. Indeed, for the parasitoid population, the kurtosis values are 1.3749 (for $k = 1.011$) and 1.6360 (for $k = 1.0093$), which are much smaller than 3. This confirms that the observed irregular behaviour in parasitoids is not indicative of on–off intermittency.

2.3. Reactivity as a route to intermittency

In a deterministic framework, the exploration of reactivity is of great importance in analysing how dynamical systems respond to perturbations. Transient fluctuations that occur after perturbations of stable equilibria can often push the system far from its equilibrium state. In such cases, the equilibrium is referred to as *reactive*, and the maximum growth rate of a disturbance is termed *reactivity* [25]. Reactivity is a concept that applies to both discrete-time [26] and continuous-time [26] systems. Its practical applications cover various fields [27–31], and it has also taken the form of generalized reactivity [32], which has proven to be particularly valuable in ecological contexts [33,34].

In Appendix A.4, we provide the classical definition of reactivity for an asymptotically stable fixed point $\bar{\mathbf{x}}$ in a generic deterministic discrete system (A.9). It involves the logarithm of the largest singular value of the Jacobian matrix evaluated at the

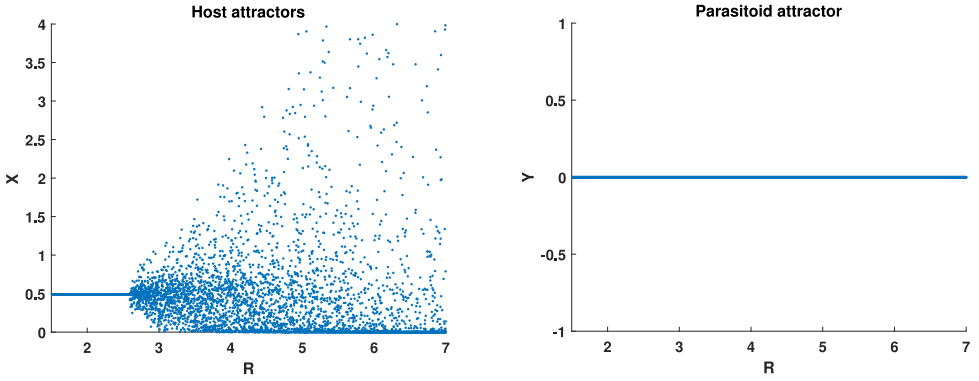

Fig. 6. Orbit diagrams for model (8) with $c = 1$, $r = 1.508$, and $k = 0.49$. Left plot: host attractors. The free-parasitoid fixed point solution $P_1 = (k, 0)$ becomes unstable at $R \approx R_c = 2.59131$ and the long-term solution transitions into a chaotic regime. Right plot: the null parasitoid attractor $Y = 0$ remains stable, regardless of the value of R.

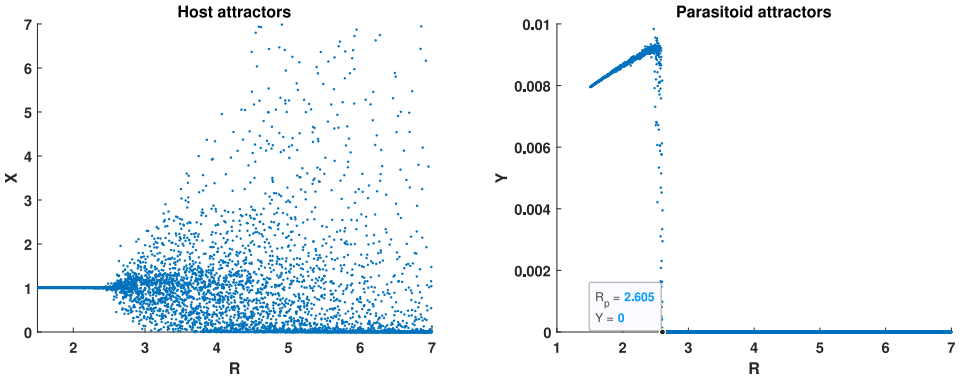

Fig. 7. Orbit diagrams for model (8) with $c = 1$, $r = 1.508$, and $k = 1.0093$. Left plot: host attractors. The free-parasitoid fixed point solution $P_1 = (k, 0)$ loses its stability when $R \approx R_c = 2.59131$, resulting in a transition to chaotic dynamics. Right plot: the null parasitoid attractor destabilizes for $R < R_p = 2.605$, while for $R \geq R_p$, the null parasitoid attractor remains stable.

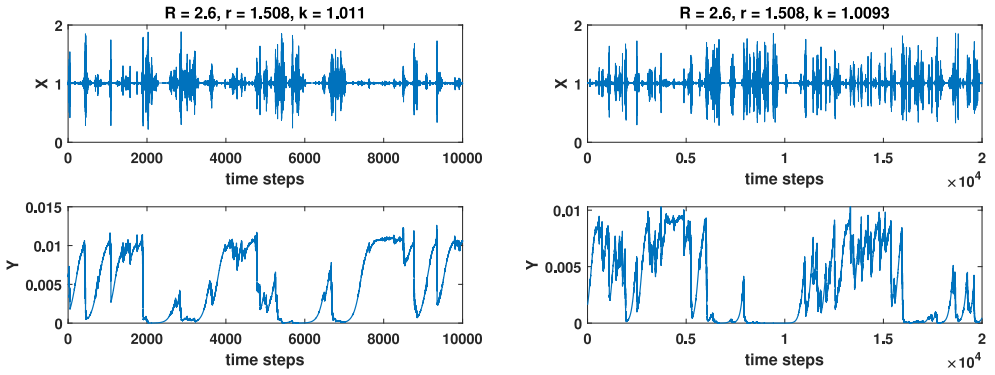

Fig. 8. Dynamics of host and parasitoid populations in the scenario with random variations in r_t. The simulation parameters are set to $c = 1$, $r = 1.508$, and $R = 2.6$ ($R_c < R < R_p$). The on–off intermittency of the host population is illustrated in the first row, while the second row shows irregular parasitoid population dynamics. The simulations cover 10^4 time steps (left panel) and $2 \cdot 10^4$ time steps (right panel) and consider two different values for k: $k = 1.011$ in the first column and $k = 1.0093$ in the second column.

fixed point, denoted as $J_{\overline{\mathbf{x}}}$. Specifically, when this logarithm is positive or, equivalently, when $\sigma_{max}(J_{\overline{\mathbf{x}}}) > 1$, the fixed point is classified as reactive. Here, we generalize the above definition of reactivity, to deal with this concept within the statistical framework.

Definition 1. Given an asymptotically stable fixed point $\overline{\mathbf{x}}$ of a stochastically parametrized discrete system, we say that $\overline{\mathbf{x}}$ is reactive (in Euclidean norm) when the phase-space average of the largest singular value of the (non-normal) Jacobian matrix evaluated at the fixed point is greater than 1.

Similarly to the deterministic case, if the Jacobian matrix is normal, then its largest singular value corresponds to the largest modulus of its eigenvalues. Therefore, the property that in correspondence of a normal Jacobian matrix a fixed point is reactive if and only if it is unstable also holds within the statistical framework.

According to the previous definition, for studying the reactivity of the free-parasitoid fixed point $P_1 = (k, 0)$ of the discrete system (8), we evaluate the largest singular value of the Jacobian matrix in (9), given by

$$\sigma(J_1^{(\epsilon)}) = \frac{\sqrt{2}}{2}\sqrt{(1-r_\epsilon)^2 + (c^2+1)\,k^2 + \sqrt{\Delta_{r_\epsilon}}},$$

where $\Delta_{r_\epsilon} = (1-r_\epsilon)^4 + k^4\,(c^2+1)^2 + 2\,k^2\,(c^2-1)\,(1-r_\epsilon)^2$ and $r_\epsilon = r + (R-r)\epsilon$. We have that $\langle\sigma(J_1^{(\epsilon)})\rangle > 1$ when

$$\int_0^1 \sigma(J_1^{(\epsilon)})\, d\epsilon > 1.$$

Hence, the reactivity curve, defined by the values that satisfy $\langle\sigma(J_1^{(\epsilon)})\rangle = 1$, can be expressed as follows:

$$\int_0^1 \sqrt{(1-r-(R-r)\epsilon)^2 + (c^2+1)\,k^2 + \sqrt{\Delta_{r+(R-r)\epsilon}}}\, d\epsilon = \sqrt{2}. \tag{11}$$

In Fig. 9, the reactivity zone of P_1 is delimited by the reactivity curve (11), represented by a green line in the parameter plane where $R > r$, for $k = 0.49$ and different values of c. Below the green line the fixed point is not reactive. In the same figure, we display the stability curve (red line) for P_1 as defined in (10) together with the kurtosis values of the host population. The region between the two curves represents the parameter space where P_1 remains both stable and reactive. It is evident that the region where the kurtosis exceeds 3 is in close proximity to the stability curve of the fixed point P_1.

The same observation was previously made for the fixed point P_0, when considering variations in δ_t (see Fig. 1). In that scenario, the reactivity curve for P_0 coincides with its stability curve, because the Jacobian matrix in (6) is diagonal, making it a normal matrix.

In the scenario with r_t varying, shown in Fig. 9, it is worth noting that, when the parameter r reaches a sufficiently high value, the region where the kurtosis (of the host population) exceeds 3 extends into the stability zone of P_1, where P_1 is reactive. As a result, plots in Fig. 9 provide the first numerical evidence that on–off intermittency can emerge even before the fixed point destabilizes, occurring within the region where the equilibrium remains stable yet reactive. To verify the onset of on–off intermittency, we consider $r = 1.508$ and $R = 2.58 < R_c$, for which P_1 is stable and reactive (the reactivity is 2.11916). In the left panel of Fig. 10 we show the temporal behaviour of the host population, that exhibits intermittency. The kurtosis is $1368.9 \gg 3$, indicating the presence of on–off intermittency. Moreover, in the same figure, we show the power spectrum (center panel) and the distribution of the off phases (right panel). All statistical quantities confirm the onset of on–off intermittency.

Our simulations support the idea that fixed point's reactivity can serve as a route to the emergence of on–off intermittency. This perspective emphasizes a dynamic aspect that warrants further exploration in future research.

3. Propagation of intermittency in coupled host-parasitoid systems

In this last section, we analyse the propagation of intermittency in a network of coupled Beddington-Free-Lawton discrete systems. We exploit the complex ecological networks formalism which provides a useful abstraction of ecological systems, representing them as graphs, composed of nodes (species) and edges (interactions). We want to analyse the contribution of networks in clarifying ecosystem properties and functioning, in terms of transmission of climate and environmental variability among species. Notice that our approach departs from the one in [18,21] where maps (instead of variables) are locally connected. The use of a complex network comprising Beddington-Free-Lawton discrete maps for modelling host-parasitoid interactions, that is beyond reach a single population dynamics, underscores our innovative approach to characterize on–off intermittency in ecological systems.

Suppose we have M interacting host-parasitoid population $(X_t^{(i)}, Y_t^{(i)})$ on a regular network. Consider a ring topology, where each node is coupled to its $L < M$ neighbours to the left, so every node has degree L. With linear host-parasitoid coupling, the dynamics is given by

$$\begin{aligned} X_{t+1}^{(i)} &= f_X^{(i)} + \sigma \sum_{j=1}^{L} \left(Y_t^{(i+j)} - X_t^{(i)} \right) \\ Y_{t+1}^{(i)} &= f_Y^{(i)} + \sigma \sum_{j=1}^{L} (X_t^{(i+j)} - Y_t^{(i)}) \end{aligned} \tag{12}$$

for $i = 1, \ldots, M$. Assuming for the network a ring structure, we set $X_t^{(M+j)} := X_t^{(j)}$, $Y_t^{(M+j)} := Y_t^{(j)}$ for $j = 1, \ldots, L$.

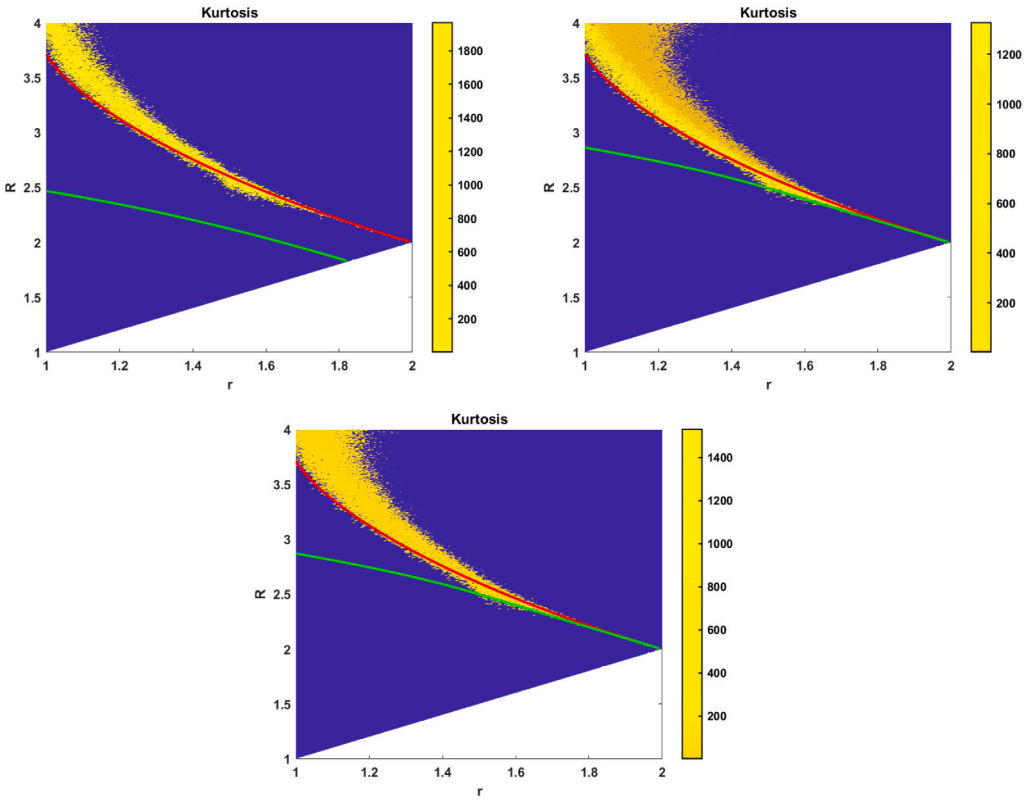

Fig. 9. r_t randomly varying. The reactivity zone of P_1 delineated by the green curve (11) in the parameter plane $R > r$, for $k = 0.49$ and values of $c = 1, 0.1, 0.01$. Below the green curve, the fixed point is non-reactive. The figure shows the stability curve (red line) for P_1 as defined in (10), together with the kurtosis values (of the host population). As r increases, the region with kurtosis (of the host population) exceeding 3 invades the zone of reactivity of the stable fixed point P_1, delimited by the green line. This numerical evidence suggests that on–off intermittency can emerge even before the fixed point destabilizes, within a region where the equilibrium remains stable yet reactive.

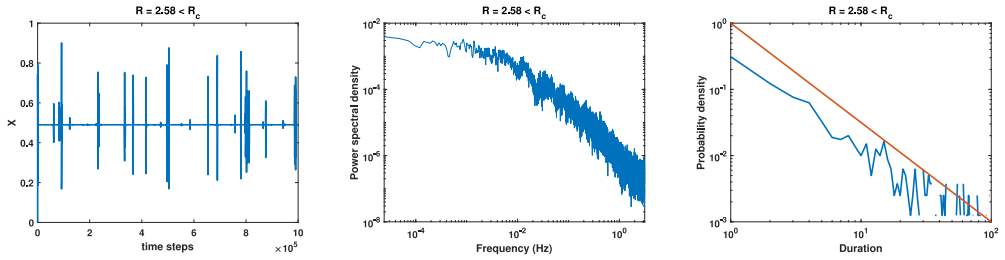

Fig. 10. r_t randomly varying. On the left, the host population X exhibits intermittent behaviour over a duration of 10^6 time steps. Parameter values are $c = 1$, $r = 1.508$, and $k = 0.49$. The value of parameter $R = 2.58 < R_c$ assures that the fixed point P_1 remains both stable and reactive. The statistical verification of on–off intermittency for the host population is also presented: in the middle, the power spectrum is shown, and on the right, the distribution of the off phases is depicted. The calculated kurtosis value is 35.28. These three statistical tools confirm the presence of on–off intermittency in the host population dynamics, centered around the stable and reactive fixed point P_1.

3.1. Intermittency driven by δ_t

In this case, we suppose that the first $M-1$ populations follow a deterministic evolution corresponding to $f_X^{(i)} := f_X(X_t^{(i)}, Y_t^{(i)})$ and $f_Y^{(i)} := f_Y(X_t^{(i)}, Y_t^{(i)})$, defined by the right hand sides of Eq. (A.2), for $i = 1, \dots, M-1$. The parameters ($c = 1$, $k = 4.9$, $r = 3$, $\delta = 0.0025701$, $k_r = 1.6\overline{3}$ and $\rho = r + \ln(\delta) = -2.9638(<0)$) are chosen in order to assure the stability of the extinction fixed point P_0. The last M-th population, instead, evolves according to a random dynamics driven by δ with $f_X^{(M)}$, $f_Y^{(M)}$ defined by the right hand sides of Eq. (5). The parameters ($\delta = 0.0025701$, $D = 0.13$, $\rho_t = 3 + \ln(\delta_t) = 3 + \ln(\delta + (D - \delta)\epsilon_t)$) are chosen in order to assure the

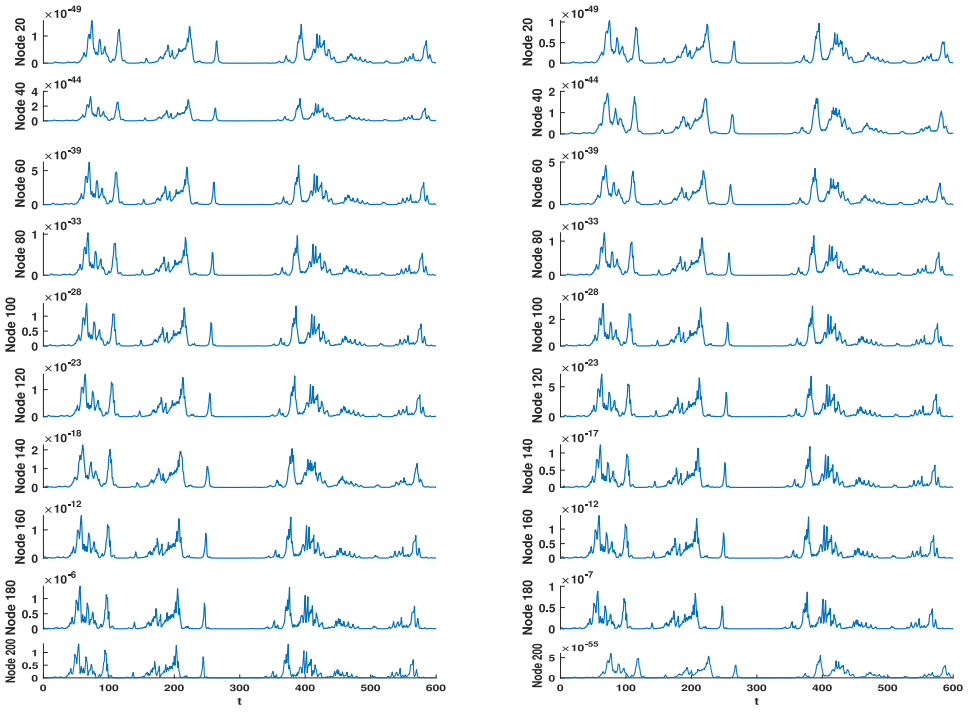

Fig. 11. Intermittency driven by δ_t on a network of $M = 200$ nodes with host-parasitoid coupling and $\sigma = 0.001$. The plots show the population evolution in selected nodes of the networks over a duration of 600 time steps. The first one (row 1) corresponds to the 20-th node, the lowest one (row 10) corresponds to the 200-th node. The other m-th rows with $m = 2, 3, \ldots, 9$ correspond to the $20m$-th node of the network. The intermittent behaviour suddenly propagates in the network, affecting not only the host population (on the left) but also the parasitoid population (on the right).

onset of the on–off intermittency. We perform a numerical investigation on the propagation of on–off intermittency in a network corresponding to $M = 200$ and $L = 10$.

When $\sigma = 0$, the maps are decoupled and, given the chosen parameters δ and D, only the host population of the randomly-driven map undergoes on–off intermittency, while the other deterministic maps tend to a stable zero solution ($\rho < 0$). For $\sigma = 0.001$ the intermittent behaviour suddenly propagates in the network, affecting not only the host population (Fig. 11, left) but also the parasitoid population (see Fig. 11, right). In this Figure we can also see a shift (in time) from last row (corresponding to the M-th node) to the first row (corresponding to the 10-th node) this indicating that intermittency also propagates over time. The same behaviour is also evident if we increase the value of σ to 0.0085 (see Fig. 12) and 0.009 (see Fig. 13). However, increasing the coupling parameter to $\sigma = 0.01$ leads to a situation where the intermittent behaviour tends to disappear, as shown in Fig. 14.

3.2. Intermittency driven by r_t

In this case, the quantities $f_X^{(i)}$ and $f_Y^{(i)}$, for $i = 1, \ldots, M-1$, represent deterministic dynamics defined by the right hand sides of Eq. (A.2), with parameter values that assure the stability of the free-parasitoid fixed point ($c = 1$, $k = 0.49$, $r = 1.508$, $\delta = 1$, $k_r = 0.3249$ and $\rho = r + \ln(\delta) = r$) , while $f_X^{(M)}$, $f_Y^{(M)}$ are defined by the right hand sides of Eq. (8) which provide a random dynamics driven by r_t, with parameters that assure the onset of on–off intermittency ($r = 1.508$, $R = 2.6$, $r_t = r + (R - r)\epsilon_t = 1.508 + 1.092\epsilon_t$). Again, we perform a numerical investigation of the propagation of intermittency in a network with $M = 200$, $L = 10$.

When $\sigma = 0$ the maps are decoupled and, given the chosen parameters r and R, only the last map undergoes intermittency, while the others tend to a stable $P_1 = (0.49, 0)$ solution. For increasing values of σ, the intermittent behaviour affects also the parasitoid population and it propagates across the nodes, see Fig. 15 for $\sigma = 0.01$. At $\sigma = 0.06$ the intermittent behaviour affects all nodes in the network, see Fig. 16. We recall that the value of σ represents the intensity of the interaction between populations. Hence, in contrast to the case of intermittency driven by δ, when intermittency is driven by changes in r, increasing the interaction intensity between populations leads to more and more nodes (populations) exhibiting on–off intermittency.

4. Discussion and conclusions

On–off intermittency is a bursting behaviour that has been proposed as a conceptual description for various natural systems, from the solar cycle [7,8] to earthquakes [11] to population outbreaks [16–21]. Basically, this type of dynamics is found when a "driven" system with an equilibrium solution (in the simplest case, a fixed point) is parametrically perturbed by another (deterministic or

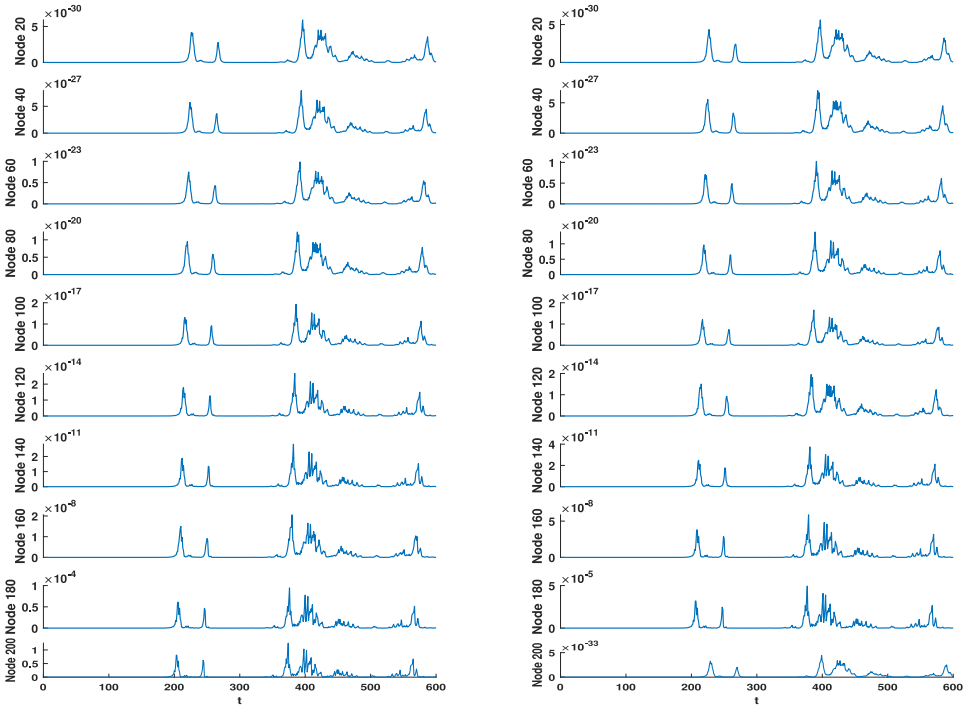

Fig. 12. Intermittency driven by δ_t on a network of $M = 200$ nodes with host-parasitoid coupling parameter $\sigma = 0.0085$. Population evolution in the same number of time steps and selected nodes of the networks of Fig. 11. As in the previous figure, intermittency propagates through the network, influencing both the host population (on the left) and the parasitoid population (on the right). Notice that this intermittency propagates not only across the nodes but also over time.

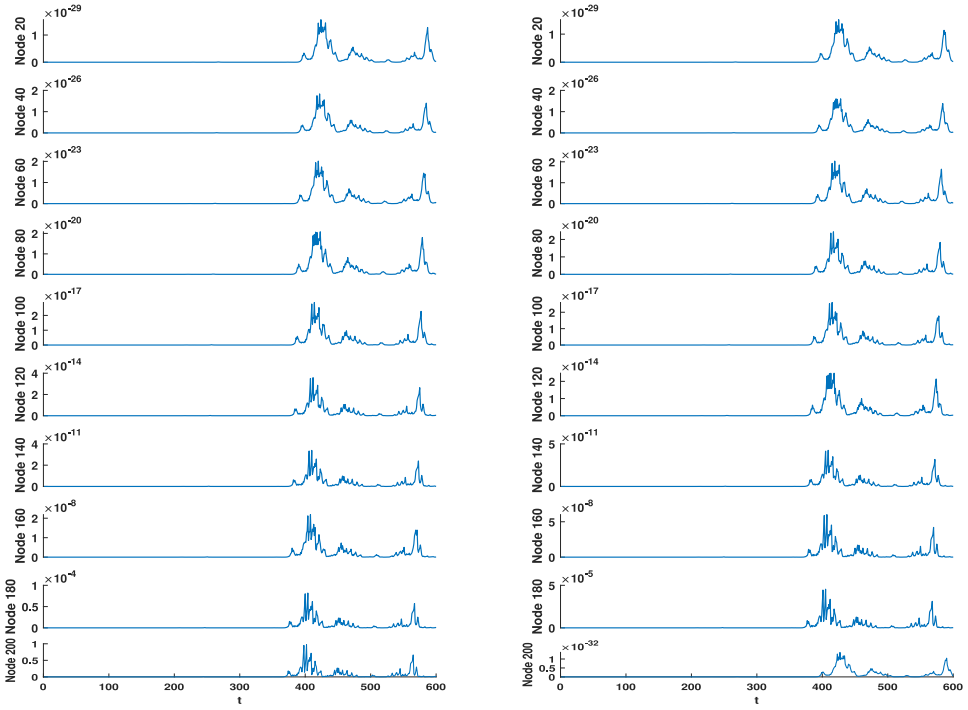

Fig. 13. Intermittency driven by δ_t on a network of $M = 200$ nodes with host-parasitoid coupling parameter $\sigma = 0.009$. Population evolution in the same number of time steps and selected nodes of the networks of Fig. 11. Increasing the coupling parameter, the intermittent behaviour tends to disappear both in host (on the left) and parasitoid (on the right) populations.

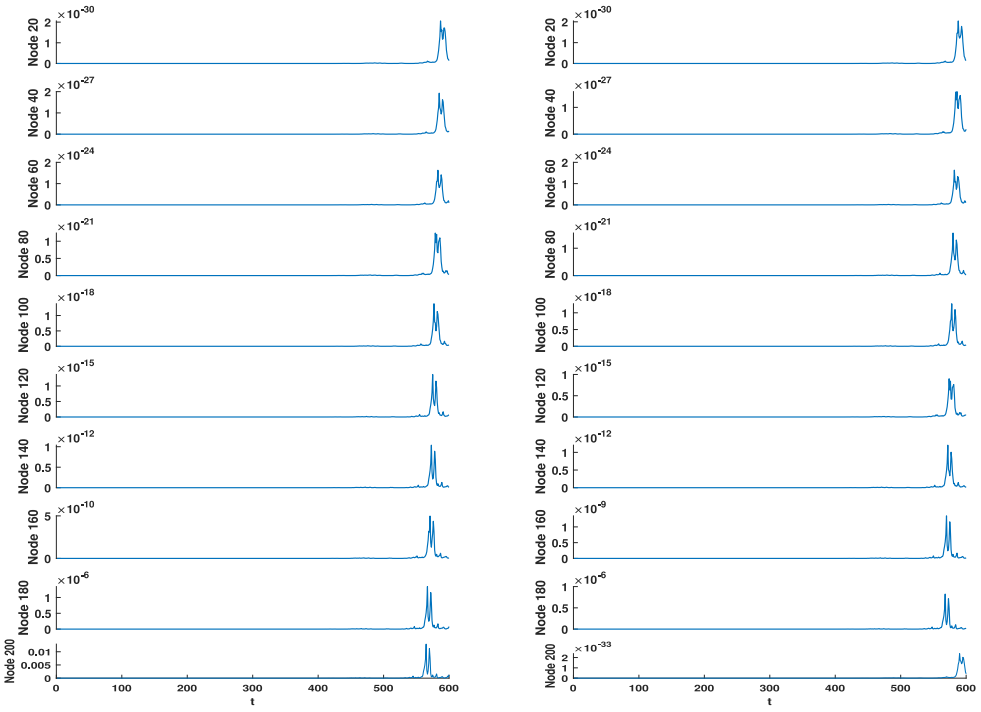

Fig. 14. Intermittency driven by δ_t on a network of $M = 200$ nodes with host-parasitoid coupling parameter $\sigma = 0.01$. Population evolution in the same number of time steps and selected nodes of the networks of Fig. 11. The intermittent behaviour is reduced to a single burst in both the host (on the left) and the parasitoid (on the right) populations.

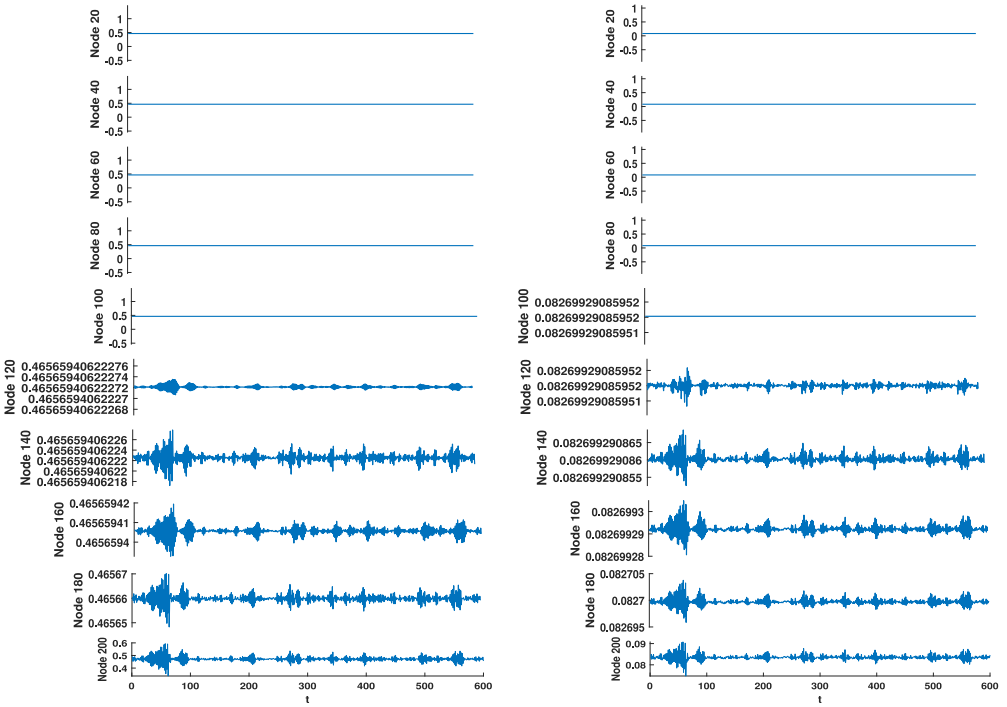

Fig. 15. Intermittency driven by r_t on a network of $M = 200$ nodes with host-parasitoid coupling and $\sigma = 0.01$. The plots show the population evolution in selected nodes of the networks over a duration of 600 time steps. The first one (row 1) corresponds to the 20-th node, the lowest one corresponds to the 200-th node. The other m-th rows with $m = 2, 3, \ldots, 9$ correspond to the $20m$-th node of the network. The intermittent behaviour slowly propagates, affecting both the host population (on the left) and the parasitoid population (on the right) in the first nodes of the network.

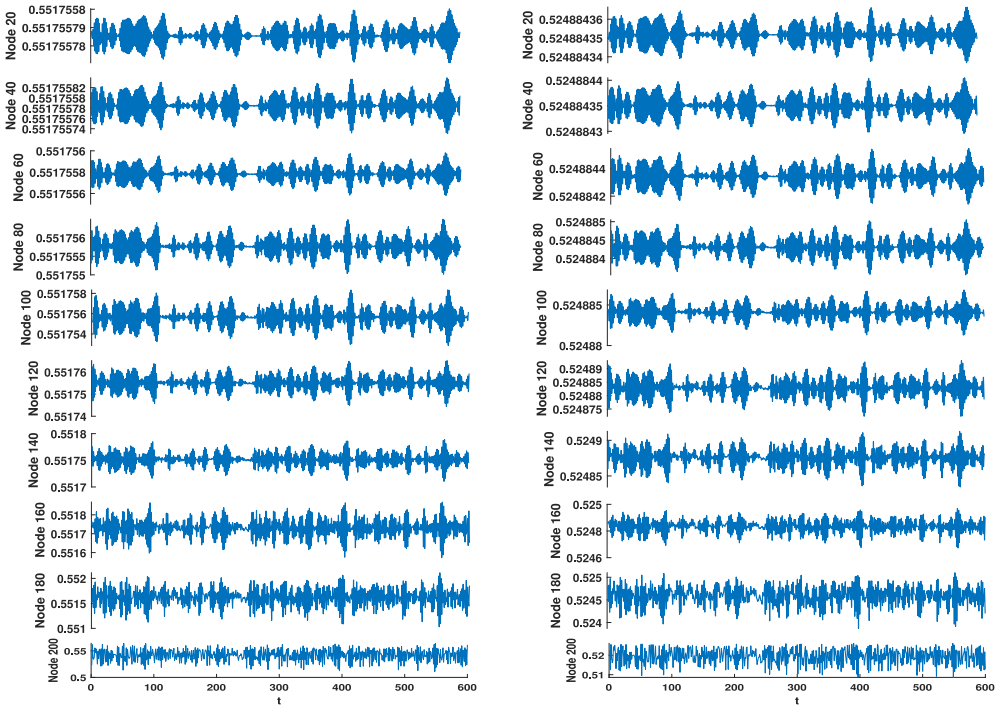

Fig. 16. Intermittency driven by r_t on a network of $M = 200$ nodes with host-parasitoid coupling and $\sigma = 0.06$. Population evolution in the same selected nodes of the networks of Fig. 15. In contrast to the case of intermittency driven by δ_t, increasing the network interaction intensity results in a higher degree of irregular intermittency behaviour.

random) system, acting as a driver, that modifies the stability properties of the equilibrium solution of the driven system. Under appropriate circumstances, the driven system displays violent excursions from the surroundings of the equilibrium solution, followed by returns towards the (same) equilibrium. In the simplest cases, the equilibrium solution does not depend on the driver and there is no feedback of the driven system on the driver, although both assumptions can be (slightly) relaxed. Interestingly, on–off intermittency is characterized by specific statistical properties, such as an approximate power-law form of the off phases and a broad, power-lawish and "red" power spectrum of the signal.

In this work, we have conducted a stability analysis of an extended version of the discrete Beddington-Free-Lawton model examined in [21]. Our model incorporates random perturbation factors that affect both the grazing intensity and the growth rate of the host population. These stochastic components play a crucial role in influencing the emergence of on–off intermittency. Expanding the analysis to incorporate multi-species interactions and trophic relationships will add complexity to the ecological model; future studies could examine how the presence of multiple species impacts the onset of on–off intermittency.

We have explored the relationship between the emergence of on–off intermittency and the novel concept of fixed point reactivity within a stochastically parametrized discrete system, from which bursting initiates. The numerical evidence presented in our simulations supports the notion that fixed point reactivity is a route for the occurrence of on–off intermittency. This perspective reveals a critical aspect of the system's dynamics that has been uncharted in earlier research, and highlights a dynamical behaviour deserving further investigation in future studies. Future research can also explore the mathematical and ecological implications of the concept of reactivity within various stochastically perturbed ecological models. This exploration may shed light on potential variations in the definition or interpretation of reactivity across diverse ecological contexts.

After studying the behaviour of an individual host-parasitoid system, this paper investigates a network of coupled host-parasitoid systems. In this network, one system is randomly perturbed in a way that generates on–off intermittency, while the others are coupled to the network but follow a deterministic dynamics. Interestingly, we found that for small but non-null coupling strengths, the on–off behaviour, driven by stochastic variation of the grazing parameter and affecting the host on a single node, propagates in the network so that the other coupled systems undergo similar bursting behaviour. However, as we increase the coupling strength, the intermittency tends to disappear. Similarly, when we induce on–off intermittency on a single node by considering stochastic variations in the growth rate intensity, this intermittent behaviour propagates throughout the network. In contrast, increasing the interaction intensity between populations leads to more and more nodes (populations) displaying on–off intermittency.

This result can be extremely interesting when considering how an environmental perturbation in just one system can rapidly affect the whole network, leading to global on–off intermittency. Unravelling the mechanisms of potential cascading effects of on–off intermittency across the network could be useful for understanding its resilience in the face of environmental perturbations. Moreover, we can explore how different coupling mechanisms impact the extent and speed of on–off intermittency propagation.

This can help identify the thresholds where behaviour shifts from local to global, providing valuable information for early warning systems. Practical applications of these findings in real-world ecological systems can design more effective pest control strategies or predict the consequences of environmental disruptions in ecosystems.

Analysing how the network's structure, including its connectivity and the roles of specific nodes, influences the propagation of bursting behaviour is another promising future investigation. Understanding the architecture that facilitates or inhibits the rapid spread of on–off intermittency can be subject of future interest.

The model represented by on–off intermittency, with its link to equilibrium reactivity, is once more a useful conceptual tool to represent bursting in natural systems, especially when considering the dynamics of coupled components. In addition, it opens up a fascinating array of future research possibilities.

CRediT authorship contribution statement

Angela Monti: Formal analysis, Investigation, Methodology, Software, Writing – original draft, Writing – review & editing. **Fasma Diele:** Formal analysis, Investigation, Methodology, Software, Writing – original draft, Writing – review & editing. **Carmela Marangi:** Writing – original draft, Writing – review & editing. **Antonello Provenzale:** Writing – original draft, Writing – review & editing.

Declaration of competing interest

The authors declare that they have no known competing financial interests or personal relationships that could have appeared to influence the work reported in this paper.

Data availability

Data will be made available on request.

Acknowledgements

We thank the Referees for their thorough reviews and helpful suggestions, which have contributed to the overall quality of the paper.

Project funded under the National Recovery and Resilience Plan (NRRP), Mission 4 Component 2 Investment 1.4 - Call for tender No. 3138 of 16 December 2021, rectified by Decree n.3175 of 18 December 2021 of Italian Ministry of University and Research funded by the European Union – NextGenerationEU; Award Number: Project code CN 00000033, Concession Decree No. 1034 of 17 June 2022 adopted by the Italian Ministry of University and Research, CUP B83C22002930006, Project title "National Biodiversity Future Center".

Fasma Diele and Angela Monti are members of GNCS INdAM. Fasma Diele and Carmela Marangi would like to thank Mr. Cosimo Grippa for his valuable technical support.

Antonello Provenzale would like to dedicate this work to the memory of Edward A Spiegel, who introduced him to on–off intermittency.

Appendix. The Beddington-Free-Lawton model

We study the local stability analysis and bifurcations of the model

$$\begin{aligned} X_{t+1} &= \delta X_t \exp\left[r\left(1-\frac{X_t}{k}\right) - c\, Y_t\right] \\ Y_{t+1} &= X_t\left[1-\exp\left(-Y_t\right)\right]. \end{aligned} \tag{A.1}$$

following the approach in [35]. Setting $\rho := r + log(\delta)$ and $k_r := k/r$, the model (3) can then be written as

$$\begin{aligned} X_{t+1} &= X_t \exp\left(\rho - \frac{X_t}{k_r} - c\, Y_t\right) \\ Y_{t+1} &= X_t\left[1-\exp\left(-Y_t\right)\right]. \end{aligned} \tag{A.2}$$

In what follows, we perform a qualitative analysis of the dynamics of this model, both for what concerns the stability and for the arising bifurcations, for variations in the parameters ρ and k_r and for a selected ensemble of fixed values of c.

A.1. Fixed points

The discrete dynamical system in (A.2) admits one extinction fixed point $P_0 = (0, 0)$, one free-parasitoid fixed point $P_1 = (\rho\, k_r, 0)$ which is positive only for $\rho > 0$, and one coexistence fixed point $P^* = (X^*, Y^*)$ that can be found by solving

$$X^* = X^* \exp\left[\rho - \frac{X^*}{k_r} - c\, Y^*\right], \qquad Y^* = X^*\left[1 - \exp(-Y^*)\right]$$

obtaining (for $X^* \neq 0$ and $Y^* \neq 0$)

$$X^* = k_r(\rho - c\, Y^*), \qquad X^* = 1/\varphi(Y^*), \qquad \varphi(y) = \frac{1 - exp(-y)}{y}.$$

Proposition 1. *A unique, strictly positive, coexistence fixed point exists for $\rho > 1/k_r$.*

Proof. A positive coexistence fixed point lies at the intersection of the straight line $x = -ck_r y + k_r\,\rho$, with negative slope $-ck_r$, and the curve $x = 1/\varphi(y)$, where $\varphi(y)$ verifies $0 < \varphi(y) < 1$ for all $y > 0$. By continuity, $x = 1/\varphi(y)$ is equal to 1 for $y = 0$ and increases for $y > 0$, while $x = -ck_r y + k_r\,\rho$ assumes value $k_r\rho$ for $y = 0$ and decreases for $y > 0$. Consequently, a strictly positive intersection may exist only if $k_r\,\rho > 1$. □

From simple geometric considerations (see left plot in Fig. A.17), it results that a positive coexistence fixed point satisfies $0 < X^* - 1 < Y^* < X^* < k_r\rho$.

Theorem 1. *The following statements hold.*

1. *If $\rho \leq 0$, then model (A.2): admits the extinction fixed point; does not admit the free-parasitoid and coexistence fixed points.*
2. *If $0 < \rho \leq \frac{1}{k_r}$, model (A.2): admits the extinction and the free-parasitoid fixed points; does not admit the coexistence fixed point.*
3. *If $\rho > \frac{1}{k_r}$, model (A.2) admits the extinction, free-parasitoid and coexistence fixed points.*

Proof. The proof easily follows by considering the free-parasitoid fixed point $P_1 = (\rho k_r, 0)$ and Proposition 1. □

A.2. Stability properties

In order to study the stability properties of the fixed points, we consider the Jacobian matrix for system (A.2), that has the following form

$$J = \begin{bmatrix} \left(1 - \frac{X_t}{k_r}\right)\exp\left(\rho - \frac{X_t}{k_r} - c\, Y_t\right) & -c\, X_t \exp\left(\rho - \frac{X_t}{k_r} - c\, Y_t\right) \\ 1 - \exp\left(-Y_t\right) & X_t \exp\left(-Y_t\right) \end{bmatrix}.$$

Theorem 2. *The extinction fixed point $P_0 = (0, 0)$ is*

(i) asymptotically stable, if $\rho < 0$;
(ii) a saddle point (unstable), if $\rho \geq 0$.

Proof. When evaluated at $P_0 = (0, 0)$, the Jacobian matrix reduces to

$$J_0 := J_{|P_0} = \begin{bmatrix} \exp(\rho) & 0 \\ 0 & 0 \end{bmatrix}$$

that admits as eigenvalues $\lambda_1 = \exp(\rho)$ and $\lambda_2 = 0$. Since $|\lambda_2| = 0 < 1$, P_0 is locally asymptotically stable if $|\lambda_1| < 1$ and unstable (saddle point) if $|\lambda_1| > 1$. Therefore the extinction fixed point is asymptotically stable if $\exp(\rho) < 1$, that is $\rho < 0$, and unstable if $\exp(\rho) > 1$, that is $\rho > 0$. If $\rho = 0$, then $\lambda_1 = 1$ and P_0 is a nonhyperbolic fixed point. Following the approach in [35], we apply the center manifold theorem [36] as follows. Usually, the first step consists in making a change of variables so that the fixed point coincides with origin. In this case we consider $u_t = X_t$ and $v_t = Y_t$. Taking this into account, we rewrite the system (A.2) by adding and subtracting $\lambda_1 u_t$ and $\lambda_2 v_t$ in the first and second equation, respectively. The system obtained has the following form

$$\begin{aligned} u_{t+1} &= \exp(\rho)u_t + f_1(u_t, v_t) \\ v_{t+1} &= g_1(u_t, v_t) \end{aligned} \tag{A.3}$$

where

$$f_1(u_t, v_t) = u_t \exp\left(\rho - \frac{u_t}{k_r} - c\, v_t\right) - \exp(\rho)u_t$$

and

$$g_1(u_t, v_t) = u_t\left[1 - \exp\left(-v_t\right)\right].$$

We look for the center manifold and we suppose that is represented by the curve

$$v = h(u) = \alpha u^2 + \beta u^3 + \mathcal{O}(u^4),$$

where $\alpha, \beta \in \mathbb{R}$ need to be determined. We observe that we consider at least a quadratic term (u^2) because the center manifold theorem assumes that $h(0) = h'(0) = 0$. Since $v_{t+1} = h(u_{t+1})$, we have

$$g_1(u_t, v_t) = h\left(\exp(\rho)u_t + f_1(u_t, v_t)\right).$$

To simplify the notation, in what follows we will use u, v instead of u_t, v_t. We observe that the function h satisfies

$$g_1(u, h(u)) = h\left(\exp(\rho)u + f_1(u, h(u))\right)$$

therefore we have

$$u\left[1 - \exp\left(-h(u)\right)\right] = h\left(u \exp\left(\rho - \frac{u}{k_r} - c\, h(u)\right)\right),$$

$$u\left[1 - \exp\left(-\alpha u^2 - \beta u^3\right)\right] = h\left(u \exp\left(\rho - \frac{u}{k_r} - c\alpha u^2 - c\beta u^3\right)\right).$$

We want to apply the polynomial identity test, thus we write the exponential terms by using their Taylor expansion. Neglecting the terms of $\mathcal{O}(u^4)$, we finally obtain

$$\alpha u^3 = \alpha(1+\rho)^2 u^2 + \beta(1+\rho)^3 u^3$$

that yields the unique solution $\alpha = \beta = 0$. The center manifold is given by the equation $v = h(u) = 0$. Therefore we can study the asymptotically stability of (A.2) by considering the stability of the following map

$$u \to \exp(\rho)u + f_1(u, h(u))$$

$$u \to L(u) = u \exp\left(\rho - \frac{u}{k_r}\right)$$

We compute the first derivative of $L(u)$

$$L'(u) = \exp\left(\rho - \frac{u}{k_r}\right)\left(1 - \frac{u}{k_r}\right)$$

and evaluate it at the fixed point $u = 0$,

$$L'(0) = \exp(\rho) = 1.$$

Since $L'(0) = 1$, we evaluate the second order derivative and obtain $L''(0) = -\frac{2}{k_r} \neq 0$. Then, it follows that the fixed point P_0 is unstable. □

Theorem 3. *The free-parasitoid fixed point $P_1 = (\rho k_r, 0)$ exists and is*

(i) asymptotically stable, if $0 < \rho < \min\left[\frac{1}{k_r}, 2\right]$ or $\rho = 2 < \frac{1}{k_r}$;
(ii) a saddle point, if $\min\left[\frac{1}{k_r}, 2\right] < \rho < \max\left[\frac{1}{k_r}, 2\right]$ or $\rho = 2 > \frac{1}{k_r}$ or $\rho = \frac{1}{k_r} < 2$;
(iii) an unstable node, if $\rho > \max\left[\frac{1}{k_r}, 2\right]$ or $\rho = \frac{1}{k_r} > 2$.

Proof. The Jacobian matrix at $P_1 = (\rho\, k_r, 0)$

$$J_1 := J_{|P_1} = \begin{bmatrix} 1-\rho & -\rho\, k_r\, c \\ 0 & \rho\, k_r \end{bmatrix}$$

has eigenvalues $\lambda_1 = 1 - \rho$ and $\lambda_2 = \rho\, k_r$. We recall that a fixed point is asymptotically stable if $|\lambda_i| < 1$ for $i = 1, 2$; it is a saddle point (unstable) if $|\lambda_i| > 1$ for some i and it is an unstable node if $|\lambda_i| > 1$ for $i = 1, 2$. If $|\lambda_i| = 1$, the stability properties follow by applying the center manifold theorem as in Theorem 2. □

Moreover, P_1 is reactive when the largest singular value of J_1, given by

$$\sigma(J_1) = \frac{\sqrt{2}}{2}\sqrt{(1-\rho)^2 + (c^2+1)\rho^2 k_r^2 + \sqrt{\Delta_\rho}}$$

where $\Delta_\rho = (1-\rho)^4 + (c^2+1)^2\rho^4 k_r^4 + 2\rho^2 k_r^2 (c^2-1)(1-\rho)^2$, verifies $\sigma(J_1) > 1$; vice versa it is not reactive. In Fig. A.17 we plot the stability region of P_1 for different values of ρ and k_r.

Theorem 4. *The coexistence fixed point P^* (exists and) is asymptotically stable if*

$$\max\left[\psi_3(c), 1/k_r\right] < \rho \leq \max\left[\psi_2(c), \psi_4(c)\right]$$

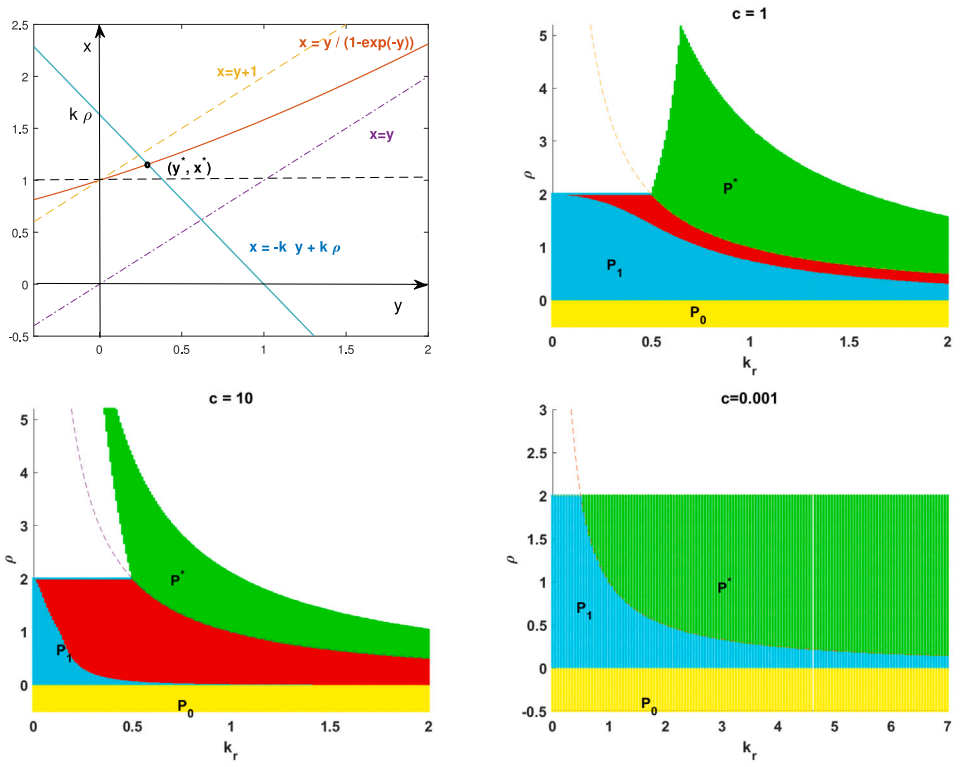

Fig. A.17. Upper left panel: geometric location of the positive coexistence fixed point for $\rho k_r > 1$. Other panels: in green the stability region of the coexistence fixed point P^*, in red the region where the free-parasitoid P_1 fixed point is stable and reactive, in cyan the region where the free-parasitoid P_1 fixed point is stable and non-reactive, in yellow the region where the extinction fixed point P_0 is stable. The values of the parameter $c = 1, 10, 0.001$ are reported on the plots.

where

$$\psi_2(c) = \frac{2 + 2X^* + 2(c-1)Y^* + cX^*Y^* - c(Y^*)^2}{1 + X^* - Y^*},$$

$$\psi_3(c) = \frac{1 - X^* - (c-1)Y^* - cX^*Y^* + c(Y^*)^2}{Y^* - X^*},$$

$$\psi_4(c) = X^* + (c-1)Y^* + 1.$$

Proof. We evaluate the Jacobian matrix at P^*

$$J^* := J_{|P^*} = \begin{bmatrix} 1 - \rho + cY^* & -cX^* \\ \frac{Y^*}{X^*} & X^* - Y^* \end{bmatrix}$$

and we apply the trace and determinant criterion for the stability analysis. The results follows by imposing that the fixed point is asymptotically stable when $|tr(J^*)| - 1 < det(J^*) < 1$, where $tr(J^*) = 1 - \rho + X^* + (c-1)Y^*$ and $det(J^*) = (1 - \rho + cY^*)(X^* - Y^*) + cY^*$. In what follows, we report only a sketch of the calculations.

- Solve $|tr(J^*)| - 1 < det(J^*)$;
  - if $tr(J^*) \geq 0$, then we solve the system

$$\begin{cases} tr(J^*) \leq 0 \\ tr(J^*) - 1 < det(J^*) \end{cases}$$

that is

$$\begin{cases} \rho \leq X^* + (c-1)Y^* + 1 = \psi_4(c) \\ \rho > \frac{c\,(X^*Y^* - (Y^*)^2)}{X^* - Y^* - 1} = c\,\psi_1 \end{cases}$$

and the unique solution is

$$c\psi_1 < \rho \leq \psi_4(c)\,; \tag{A.4}$$

– if $tr(J^*) < 0$, then we obtain the system

$$\begin{cases} tr(J^*) < 0 \\ -tr(J^*) - 1 < det(J^*) \end{cases}$$

that is

$$\begin{cases} \rho > X^* + (c-1)Y^* + 1 = \psi_4(c) \\ \rho < \frac{2+2X^*+2(c-1)Y^*+cX^*Y^*-c(Y^*)^2}{1+X^*-Y^*} = c\,\psi_2(c) \end{cases}$$

and the unique solution is

$$\psi_4(c) < \rho < \psi_2(c)\,. \tag{A.5}$$

The solution of $|tr(J^*)| - 1 < det(J^*)$ is given by the union of (A.4) and (A.5), that yields to

$$\min\left[c\,\psi_1, \psi_4(c)\right] < \rho < \max\left[\psi_2(c), \psi_4(c)\right]. \tag{A.6}$$

- Solve $det(J^*) < 1$, which solution is

$$\rho > \frac{1 - X^* - (c-1)Y^* - cX^*Y^* + c(Y^*)^2}{Y^* - X^*} = \psi_3(c) \tag{A.7}$$

- Finally, the solution of $|tr(J^*)| - 1 < det(J^*) < 1$ is obtained by the intersection of (A.6) and (A.7), that is

$$\max\left\{\min\left[c\,\psi_1, \psi_4(c)\right], \psi_3(c)\right\} < \rho < \max\left[\psi_2(c), \psi_4(c)\right]. \tag{A.8}$$

- At last, we guarantee the existence of the fixed point, therefore we intersect (A.8) with the existence condition $\rho > \frac{1}{k_r}$ given in Proposition 1. Thus we obtain

$$\max\left\{\min\left[c\,\psi_1, \psi_4(c)\right], \psi_3(c), \frac{1}{k_r}\right\} < \rho < \max\left[\psi_2(c), \psi_4(c)\right].$$

As shown in Fig. A.17, a positive coexistence fixed point satisfies $0 < X^* - 1 < Y^* < X^* < k_r\rho$. As a consequence $c\psi_1 < 0$, so that $\min\left[c\,\psi_1, \psi_4(c)\right] < 0$ and, since $k_r > 0$, we have that $\max\left\{\min\left[c\,\psi_1, \psi_4(c)\right], \psi_3(c), \frac{1}{k_r}\right\} = \max\left[\psi_3(c), \frac{1}{k_r}\right]$. □

The results of a numerical investigation about stability properties of the coexistence fixed point are reported in Fig. A.17 for $c = 1, 10, 0.001$.

A.3. Bifurcation analysis and intermittent behaviour

We briefly recall the different types of bifurcation that may occur at fixed points.

Remark 1. A saddle–node bifurcation occurs when the Jacobian matrix has an eigenvalue equal to 1 and the other inside the unit circle.

Remark 2. A period-doubling bifurcation occurs when the Jacobian matrix has an eigenvalue equal to −1 and the other inside the unit circle.

Remark 3. A Neimark–Sacker bifurcation occurs when the Jacobian matrix has two complex conjugate eigenvalues on the unit circle.

Theorem 5. *A saddle–node bifurcation occurs at the extinction fixed point, if* $\rho = 0$.

Proof. See Remark 1. □

Theorem 6. *At the free-parasitoid fixed point,*

(i) a period-doubling bifurcation occurs if $\rho = 2$ *and* $k_r < \frac{1}{2}$;
(ii) a saddle–node bifurcation occurs, if $\rho = \frac{1}{k_r}$ *and* $k_r > \frac{1}{2}$.

Proof. See Remarks 2 and 1. □

Theorem 7. *At the coexistence fixed point,*

1. *a Neimark–Sacker bifurcation occurs, if* $\rho = \psi_3(c)$ *and* $\psi_5(c) < \rho < \psi_6(c)$ *where* $\psi_5(c) = -1 + X^* + (c-1)Y^*$ *and* $\psi_6(c) = 3 + X^* + (c-1)Y^*$;
2. *a period-doubling bifurcation occurs if,* $\rho = \psi_2(c)$.

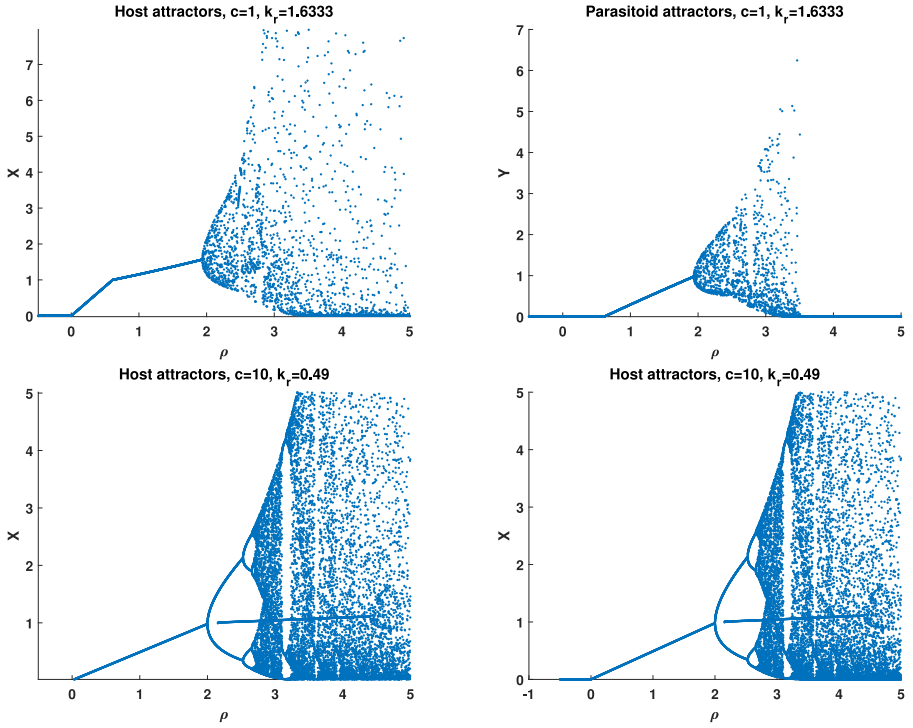

Fig. A.18. Orbit diagrams depicting attractors with respect to $\rho < 5$, for $k_r = 1.6\overline{3}$ and $c = 1$ (first row) and, for $k_r = 0.3$ and $c = 10$ (second row, on the right) and $c = 10$ and $k_r = 0.49$ (second row, on the left). It is possible to recognize the Neimark–Sacker bifurcation at the coexistence fixed point (first row) and a period-doubling bifurcation at the free-parasitoid fixed point (second row).

Proof. By considering Remarks 3 and 2, we apply the trace and determinant criteria. Therefore, we have a Neimark–Sacker bifurcation if

$$det(J^*) = 1 \; and \; |tr(J^*)| < 2.$$

A period-doubling bifurcation occurs if

$$1 + tr(J^*) + det(J^*) = 0. \quad \square$$

Orbit diagrams in Fig. A.18, depicting the long run-behaviour starting from $X_0 = 1.1966$ and $Y_0 = 0.3703$, show X and Y attractors for $-0.5 < \rho < 5$. We can recognize an example of Neimark–Sacker bifurcation at the coexistence fixed point and a period-doubling bifurcations at the free-parasitoid fixed point.

Finally, the numerical evaluation of the maximum Lyapunov exponent (A.11), plotted in Fig. A.19 as a function of the parameter ρ, indicates the route to chaos. We show two examples of onset of chaotic intermittency in the Beddington-Free-Lawton model: for $c = 1$ and $k_r = 1.6\overline{3}$ intermittency is detected at $\rho \approx 2.57811$ (see Fig. A.20 on the left); for $c = 10$ and $k_r = 0.3$ intermittency of solely host population can be seen at $\rho \approx 2.781595$ (see Fig. A.20 on the right). Notice that this type of intermittent behaviour is not on–off intermittency, which we discuss below.

A.4. Reactivity, resilience and Lyapunov exponents

Consider the discrete system (or maps)

$$\mathbf{x}(t+1) = \mathbf{f}(\mathbf{x}(t)). \tag{A.9}$$

A.4.1. Stability

To study the stability of a fixed point $\overline{\mathbf{x}}$, we analyse the stability of the null equilibrium of the linearized system at $\overline{\mathbf{x}}$. Let $J^{(i)}_{\overline{\mathbf{x}}} = \left(\frac{\partial \mathbf{f}(\mathbf{x}(i))}{\partial \mathbf{x}(i)}\right)_{|\mathbf{x}(i)=\overline{\mathbf{x}}}$ so that the linearization of the system (A.9) at $\overline{\mathbf{x}}$ is given by

$$\eta(t) = J^{(t-1)}_{\overline{\mathbf{x}}}\eta(t-1) = \ldots = \overset{\curvearrowleft}{\prod_{i=0}^{t-1}} J^{(i)}_{\overline{\mathbf{x}}}\,\eta(0) = H_{t,\overline{\mathbf{x}}}\,\eta(0).$$

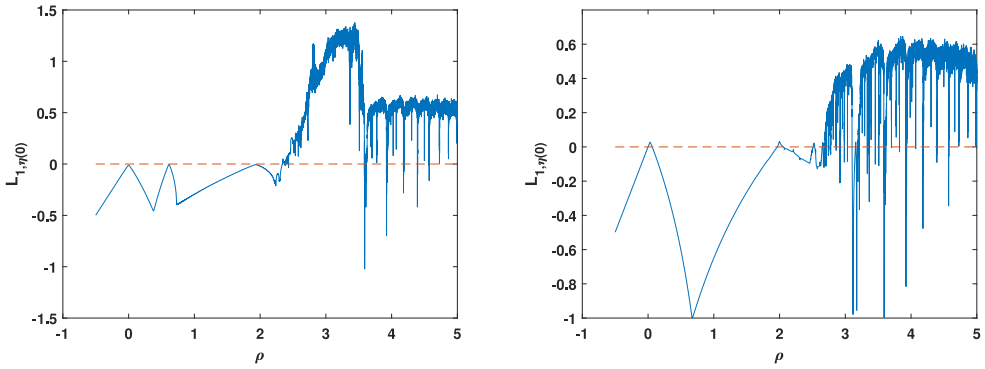

Fig. A.19. Maximum Lyapunov exponent $L_{1,\eta(0)}$ for $\eta(0) = (2.44194, 0.528998)$, $k_r = 1.6\overline{3}$, $c = 1$. The maximum Lyapunov exponent is plotted against ρ for $c = 1$, $k_r = 1.6\overline{3}$ on the left and $c = 10$, $k_r = 0.49$ on the right.

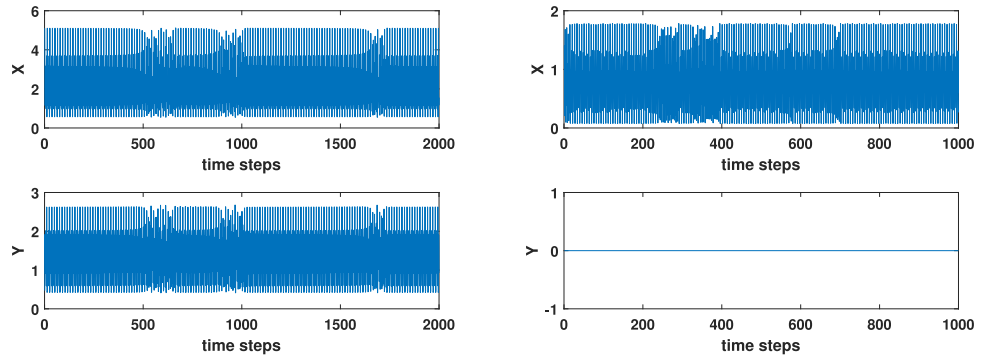

Fig. A.20. Intermittent behaviour of both host and parasitoid populations is observed at $\rho \approx 2.57811$ for $c = 1$ and $k_r = 1.6\overline{3}$ (on the left); the arising of host population intermittency is detected at $\rho \approx 2.781595$ for $c = 10$ and $k_r = 0.3$ (on the right).

The long-term behaviour of $\eta(t)$ is determined by the spectral radius $\psi(H_{t,\bar{\mathbf{x}}})$ of the matrix $H_{t,\bar{\mathbf{x}}}$ (i.e. the maximum of the modulus of its eigenvalues).

A.4.2. Amplification envelope, reactivity and resilience

Suppose $\bar{\mathbf{x}}$ asymptotically stable (and assume that the Jacobian is not normal to neglect the trivial case). In [26], the *amplification envelope* has been defined as

$$\phi(t) := \max_{\|\eta(0)\|\neq\mathbf{0}} \frac{\|\eta(t)\|}{\|\eta(0)\|} = \max_{\|\eta(0)\|\neq\mathbf{0}} \frac{\|H_{t,\bar{\mathbf{x}}}\,\eta(0)\|}{\|\eta(0)\|} = |||H_{t,\bar{\mathbf{x}}}|||.$$

When $\|\cdot\|$ is the Euclidean norm, then the induced norm $|||\cdot|||$ is the spectral norm and

$$\phi(t) = \phi_2(t) := \sqrt{\psi(H^T_{t,\bar{\mathbf{x}}}\,H_{t,\bar{\mathbf{x}}})} = \sigma_{max}(H_{t,\bar{\mathbf{x}}}), \tag{A.10}$$

where σ_{max} is the largest singular value of the matrix $H_{t,\bar{\mathbf{x}}}$.

Denote $r(t) := \ln \phi_2(t)$; the maximum rate of departure from $\bar{\mathbf{x}}$ immediately following a perturbation $\eta(0)$ can be evaluated as $r(1) = \ln \phi_2(1) = \ln[\sigma_{max}(J^{(0)}_{\bar{\mathbf{x}}})]$. When $r(1) > 0$ then the system is called *reactive*.

The *resilience* of $\bar{\mathbf{x}}$ is defined as

$$L_{1,\bar{\mathbf{x}}} := \lim_{t\to\infty} \frac{1}{t}\, r(t) = \lim_{t\to\infty} \frac{1}{t} \ln \sqrt{\psi(H^T_{t,\bar{\mathbf{x}}}\,H_{t,\bar{\mathbf{x}}})} = \lim_{t\to\infty} \frac{1}{t} \ln \sigma_{max}(H_{t,\bar{\mathbf{x}}}).$$

A.4.3. The maximum Lyapunov exponent

The maximum Lyapunov exponent $L_{1,\eta(0)}$ determines whether, starting from $\eta(0)$, two infinitely close trajectories move away from, or approach, each other. By definition, it results that

$$L_{1,\eta(0)} = \lim_{t\to\infty} \frac{1}{t} \ln \sqrt{\psi(H^T_{t,\eta(0)}\,H_{t,\eta(0)})} \tag{A.11}$$

i.e. the maximum Lyapunov exponent is a measure of the resilience of a perturbation $\eta(0)$.

References

[1] Pomeau Y, Manneville P. Intermittent transition to turbulence in dissipative dynamical systems. Comm Math Phys 1980;74:189–97.
[2] Elaskar S, Del Río E. New advances on chaotic intermittency and its applications. Springer; 2017.
[3] Ott E. Chaos in dynamical systems. Cambridge University Press; 2002.
[4] Fujisaka H, Yamada T. A new intermittency in coupled dynamical systems. Progr Theoret Phys 1985;74(4):918–21.
[5] Platt N, Spiegel E, Tresser C. On-off intermittency: A mechanism for bursting. Phys Rev Lett 1993;70(3):279.
[6] Heagy J, Platt N, Hammel S. Characterization of on-off intermittency. Phys Rev E 1994;49(2):1140.
[7] Platt N, Spiegel EA, Tresser C. The intermittent solar cycle. Geophys Astrophys Fluid Dyn 1993;73(1–4):147–61.
[8] Spiegel EA. Chaos and intermittency in the solar cycle. Orig Dyn Sol Magn 2009;25–51.
[9] Cabrera JL, Milton JG. On-off intermittency in a human balancing task. Phys Rev Lett 2002;89(15):158702.
[10] Hramov A, Koronovskii AA, Midzyanovskaya I, Sitnikova E, Van Rijn C. On-off intermittency in time series of spontaneous paroxysmal activity in rats with genetic absence epilepsy. CHAOS 2006;16(4).
[11] Bottiglieri M, Godano C. On-off intermittency in earthquake occurrence. Phys Rev E 2007;75:026101.
[12] Hammer PW, Platt N, Hammel SM, Heagy JF, Lee BD. Experimental observation of on-off intermittency. Phys Rev Lett 1994;73(8):1095.
[13] von Hardenberg JG, Paparella F, Platt N, Provenzale A, Spiegel E, Tresser C. Missing motor of on-off intermittency. Phys Rev E 1997;55(1):58.
[14] Toniolo C, Provenzale A, Spiegel EA. Signature of on-off intermittency in measured signals. Phys Rev E 2002;66:066209.
[15] Metta S, Provenzale A, Spiegel EA. On–off intermittency and coherent bursting in stochastically-driven coupled maps. Chaos Solitons Fractals 2010;43(1):8–14.
[16] Ferriere R, Cazelles B. Universal power laws govern intermittent rarity in communities of interacting species. Ecology 1999;80(5):1505–21.
[17] De Feo O, Ferriere R. Bifurcations analysis of population invasion: on–off intermittency and basin riddling. Int J Bifurcation Chaos 2000;10(02):443–52.
[18] Moon W. On-off intermittency in locally coupled maps. Woods Hole Oceanographic Institution MA; 2010.
[19] Sharma Y, Abbott KC, Dutta PS, Gupta AK. Stochasticity and bistability in insect outbreak dynamics. Theor Ecol 2015;8:163–74.
[20] Vissio G, Provenzale A. On-off intermittency in a three-species food chain. Mathematics 2021;9(14).
[21] Vissio G, Provenzale A. On-off intermittency and irruptions in host-parasitoid dynamics. J Theoret Biol 2022;111174.
[22] Turchin P. Complex population dynamics, a theoretical/empirical synthesis (MPB-35). Princeton: Princeton University Press; 2003.
[23] Beddington J, Free C, Lawton J. Concepts of stability and resilience in predator–prey models. J Anim Ecol 1976;791–816.
[24] Schowalter TD. Insect ecology: an ecosystem approach. Academic Press; 2022.
[25] Neubert MG, Caswell H. Alternatives to resilience for measuring the responses of ecological systems to perturbations. Ecology 1997;78(3):653–65.
[26] Caswell H, Neubert MG. Reactivity and transient dynamics of discrete-time ecological systems. J Difference Equ Appl 2005;11(4–5):295–310.
[27] Chen X, Cohen JE. Transient dynamics and food–web complexity in the lotka–volterra cascade model. Proc R Soc B 2001;268(1469):869–77.
[28] Neubert MG, Klanjscek T, Caswell H. Reactivity and transient dynamics of predator–prey and food web models. Ecol Model 2004;179(1):29–38.
[29] Neubert MG, Caswell H, Murray J. Transient dynamics and pattern formation: reactivity is necessary for turing instabilities. Math Biosci 2002;175(1):1–11.
[30] Marvier M, Kareiva P, Neubert MG, destruction Habitat, fragmentation. And disturbance promote invasion by habitat generalists in a multispecies metapopulation. Risk Anal: Int J 2004;24(4):869–78.
[31] Hosack GR, Rossignol PA, Van Den Driessche P. The control of vector-borne disease epidemics. J Theoret Biol 2008;255(1):16–25.
[32] Mari L, Casagrandi R, Rinaldo A, Gatto M. A generalized definition of reactivity for ecological systems and the problem of transient species dynamics. Methods Ecol Evol 2017;8(11):1574–84.
[33] Diele F, Luiso I, Marangi C, Martiradonna A. Soc-reactivity analysis for a newly defined class of two-dimensional soil organic carbon dynamics. Appl Math Model 2023;118:1–21.
[34] Diele F, Luiso I, Marangi C, Martiradonna A, Woźniak E. Evaluating the impact of increasing temperatures on changes in soil organic carbon stocks: sensitivity analysis and non-standard discrete approximation. Comput Geosci 2022;26(5):1345–66.
[35] Azizi T. Local stability analysis and bifurcations of a discrete-time host-parasitoid model. Int J Mod Nonlinear Theory Appl 2020;9(02):19.
[36] Elaydi SN. Discrete chaos. Boca Raton, FL: Chapman & Hall/CRC; 2000.